# Structure-property relationship in achiral hockey stick-shaped mesogens with lateral halogen substitutions

By

**Kaveri**

*A dissertation submitted for the partial fulfilment of a BS-MS dual degree in Science*


Indian Institute of Science Education and Research Mohali

April 2019

B

# Certificate of Examination

This is to certify that the dissertation titled "**Structure-property relationship in achiral hockey stick-shaped mesogens with lateral halogen substitutions**" submitted by Kaveri (MS14154) for the partial fulfilment of BS-MS dual degree program of the Institute, has been examined by the thesis committee duly appointed by the Institute. The committee finds the work done by the candidate satisfactory and recommends that the report be accepted.

Dr. Raj Kumar Roy  Dr. Subhabrata Maiti  Dr. Santanu Kumar Pal
(Supervisor)

Dated: 24 April 2019

D

# Declaration

The work presented in this dissertation has been carried out by me under the guidance of Dr. Santanu Kumar Pal at the Indian Institute of Science Education and Research Mohali.

This work has not been submitted in part or in full for a degree, a diploma, or a fellowship to any other university or institute. Whenever contributions of others are involved, every effort is made to indicate this clearly, with due acknowledgement of collaborative research and discussions. This thesis is a bonafide record of original work done by me and all sources listed within have been detailed in the bibliography.

Kaveri

(MS14154)

Dated: 24 April 2019

In my capacity as the supervisor of the candidate's project work, I certify that the above statements by the candidate are true to the best of my knowledge.

Dr. Santanu Kumar Pal

(Supervisor)

F

# Acknowledgement

The success and final outcome of this project engrossed huge amount of work, dedication and research. Still, enacting it would had been impossible if the support of certain individuals was not there with me. On that account, I would like to take this opportunity to express my sincere gratitude towards all of them.

I cannot thank enough to my Mom, my Sister and my Brother for always being there for me and for always being supportive towards me whenever I was not able to be there for them. Its their love, affection and their trust in me that helped me to go on and stay motivated.

I respect and thank Dr. Santanu Kumar Pal, Associate Professor, Department of Chemical Sciences, Indian Institute of Science Education and Research Mohali, who gave me all his valuable guidance, support and environment to work in my own way. It was his constant encouragement which helped me to successfully finish my Master's project.

I would like to thank Dr. Raj Kumar Roy and Dr. Subhabrata Maiti, my committee members, for their critical suggestions and guidance during the committee meetings.

There are not enough words that can help to express my deep gratitude to Supreet Di, my mentor, for giving me her immeasurable guidance, support and remarks throughout my project work. She has always been patient and supportive throughout the time I was struggling with my work and has always showed trust in me. She was my constant pillar of strength and my friend whenever I needed her to be either of the two things. Without her, it would had been impossible for my work to reflect the way it did and for me to stay focused and dedicated towards my work.

I owe my sincere thanks to Dr. Golam Mohiuddin, who always took keen interest in my project work and guided me throughout the completion of it. He was always supportive and provided me with all the necessary information that could help me in overcoming the problems I was facing during my research work.

A special thanks to Vidhika Di and Neha, for always being there for me and helping me with my work whether its inside or outside the lab. They have been my constant companions who kept me sane throughout the year and always gave me innumerable suggestions to solve my problems. I

would also take this opportunity to thank Yogi for always posing constant questions at me which made me think about the problems I was facing during my work. He was the friend in need, the savior during the times and the source of guidance I was in constant need of.

I would like to thank Harpreet bhaiya and Shruti di for their motivation at different times and for all the fun I had with them during my project time.

I would take a moment to thank my fellow project students Diksha, Najiya and Abdul for their constant support and always helping me in the time of crisis. Along with this, I would also like to thank all my labmates including Nazma Mam, Manisha Mam, Indu Bala Di and Ipsita Di for always making it fun environment to work in the lab.

I would also like to thank my friends Mridul, Sakshi, Naman and Ajeet for always being my strength and support. Also, Komal, Prateek, Dipali, Neeraj and Prabhat for always being patient with me whenever I was unavailable for them and still supporting me throughout my project work. It was their constant motivation and their trust in me which helped me to accelerate my work towards completion.

Lastly, I would like to thank IISER Mohali for providing me all the infrastructure and instruments and Inspire for the fellowship.

# List of Figures

## Chapter 1: Introduction



## Chapter 2: Synthesis and Characterizationof hockey-stick shaped compounds

# List of Schemes and Tables

# Notation

| | |
|---|---|
| LC | Liquid Crystals |
| DLC | Discotic Liquid Crystals |
| BLC | Bent Liquid Crystals |
| Cr | Crystal |
| Iso | Isotropic liquid |
| N | Nematic |
| $N_b$ | Biaxial Nematic |
| $N_D$ | Discotic Nematic |
| Sm | Smectic |
| IUPAC | International Union of Pure and Applied Chemistry |
| NMR | Nuclear Magnetic Resonance |
| ATR | Attenuated Total Reflection |
| HRMS | High Resolution Mass Spectroscopy |
| POM | Polarized Optical Microscopy |
| DSC | Differential Scanning Calorimetry |
| RM | Reaction mixture |
| RB | Round Bottom |
| w.r.t. | With Respect To |
| UV | Ultra Violet |

| | |
|---|---|
| Vis | Visible |
| RT | Room Temperature |
| DFT | Density Function Theory |

# Contents

# Abstract

This thesis deals with the study of structure-property relationship in two series of achiral hockey stick-shaped molecules with different lateral halogen substitutions at the terminal polar ring. The behaviour of the halogens (X = F, Cl) at the lateral position of the short arm and the role of end alkyl chains (n = 4, 6, 8, 10, 12, 14, 16, 18) at the long arm on phase structure of the mesogens have been characterized. All the compounds are shown to exhibit enantiotropic Liquid Crystal behavior and the Liquid Crystal nature has been characterized and verified.

The first section of this thesis deals with the introduction of LCs, brief history, applications and types of LCs. The class of BLCs have been elaborated.

In the second section, the motivation of our work has been presented with detailed synthesis and characterization of all the compounds. The synthetic procedures have been mentioned and the compound's spectral and thermal behaviour has been analysed via different spectroscopic techniques. The chapter is rounded off with the conclusions and future outlook section.

# CHAPTER 1

# Introduction

## 1.1 Liquid Crystals

Liquid crystal (LCs) is an intermediate state of matter between anisotropic solids and isotropic liquids i.e. it possesses a combination of properties of both solids and liquids, as represented in figure 1. They have orientational and positional order (like solids), and fluidity (like liquids). Due to the shape anisotropy of LCs, they exhibit optical anisotropy (birefringence) as well as dielectric anisotropy.

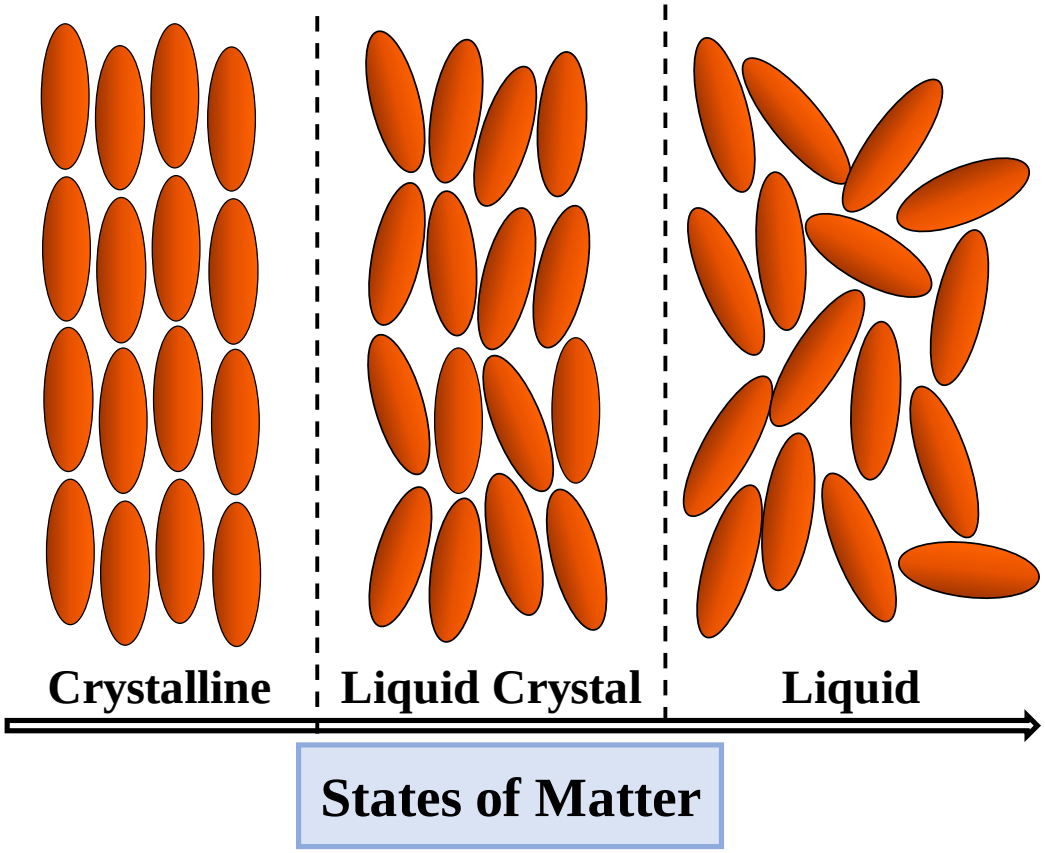


**Figure 1**: Ordering of molecules in different states of matter.

Image adapted and redrawn from: reddit, r/chemistry, liquid crystal phases under polarized light. *https://www.reddit.com/r/chemistry/comments/3vp3fd/liquid_crystal_phases_under_polarised_light/*

## 1.2 Classification of LCs

The flowchart presented in Figure 2 gives an overview of the types of LCs. The LCs are broadly categorized into two categories: Thermotropic and Lyotropic. Further Thermotropic LCs are divided into three categories depending upon the structure of mesogens: Calamitic, Discotic, and Bent-shaped LCs.

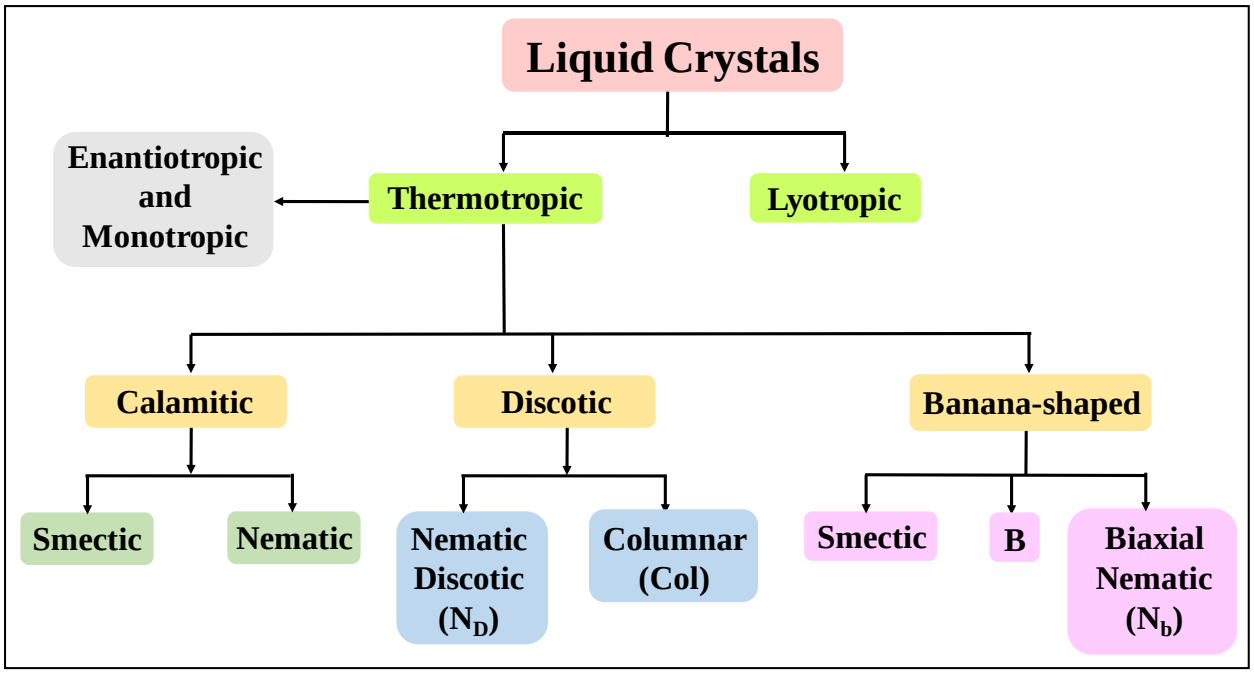


**Figure 2**: Classification of LCs

Image adapted and redrawn from: Classification and example of LCs by cleanenergywiki

*http://photonicswiki.org/index.php?title=Classification_and_Examples_of_Liquid_Crystals*

### 1.2.1 Based on the formation of mesophase

- **Thermotropic LCs:** LCs which are formed as a function of temperature.
- **Lyotropic LCs:** LCs which are formed as a function of concentration of solvent.

### 1.2.2 Based on the structure of mesophase

Based on the structure, there are three different types of LC phases which are:

- **Nematic phase** (figure 3a)
- **Cholesteric phase** (figure 3b)
- **Smectic phase** (figure 4)

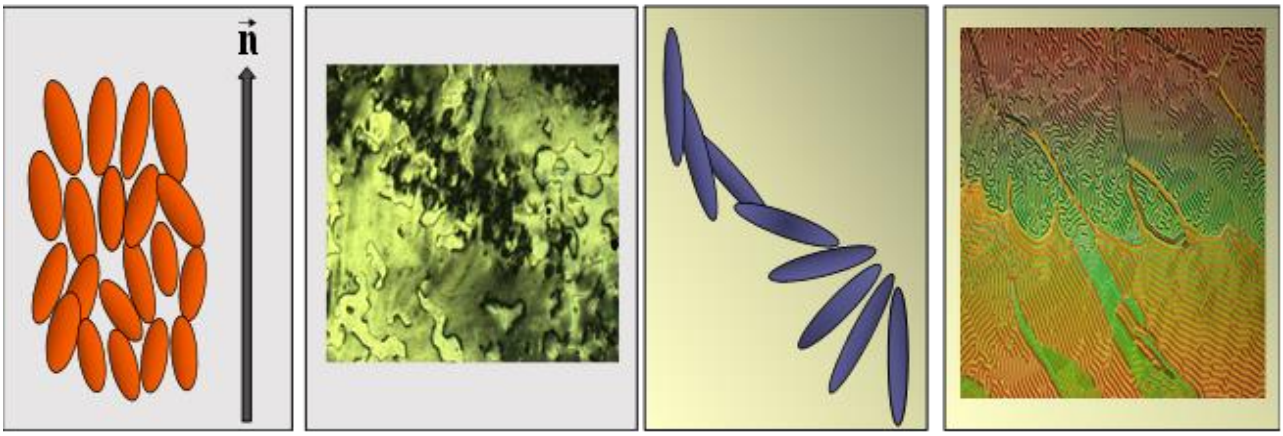


**Figure 3**: Arrangement of mesogens in (a) N phase (LHS) and (b) Cholesteric phase (RHS) with a representative Schlieren as well as Fingerprint like texture respectively.

Image adapted and redrawn from: Classification and example of LCs by cleanenergywiki

*http://photonicswiki.org/index.php?title=Classification_and_Examples_of_Liquid_Crystals*

b: (RHS) [*Cholesteric liquid crystal in a wedge cell By Dr. Ken Ishikawa*]

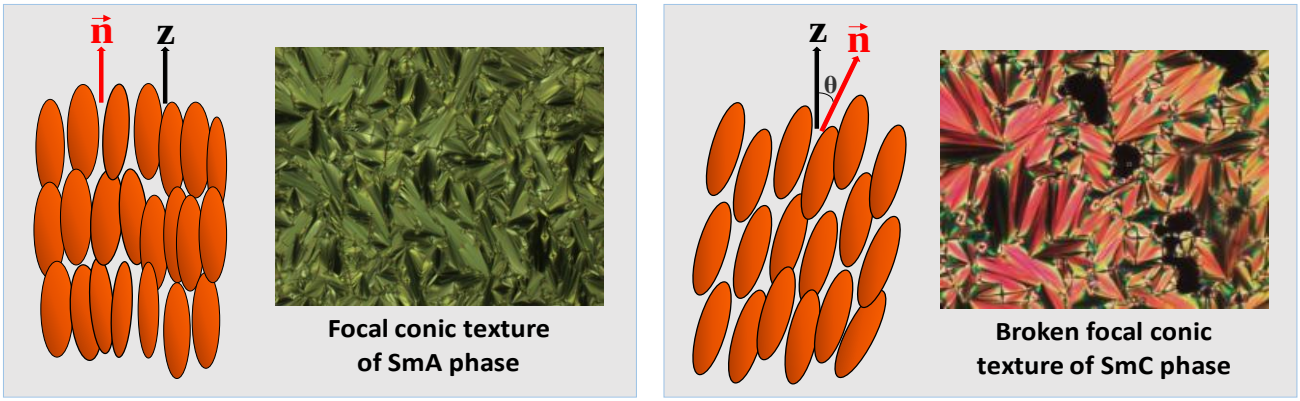


**Figure 4**: Mesogenic arrangement in (a) SmA (LHS) and (b) SmC (RHS) phases with a representative focal conic and broken focal conic texture respectively

Image adapted and redrawn from: Classification and example of LCs by cleanenergywiki

*http://photonicswiki.org/index.php?title=Classification_and_Examples_of_Liquid_Crystals*

### 1.2.3 Based on the structure of mesogens:

- **Calamitic LCs** (figure 5)

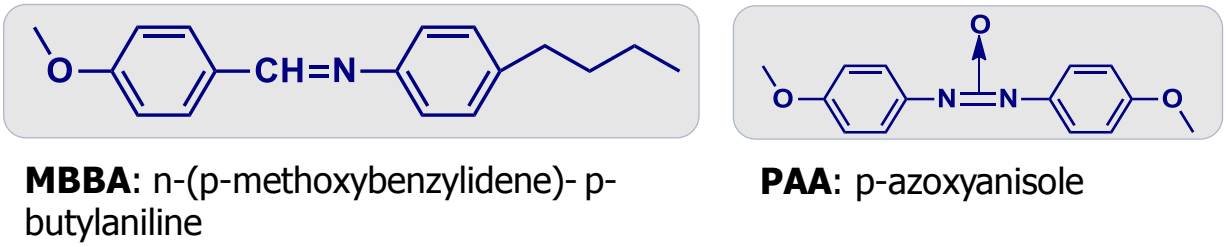


**MBBA**: n-(p-methoxybenzylidene)- p-butylaniline

**PAA**: p-azoxyanisole

**Figure 5**: Typical examples of Calamitic LCs

- **Discotic LCs (DLCs)** (figure 6)

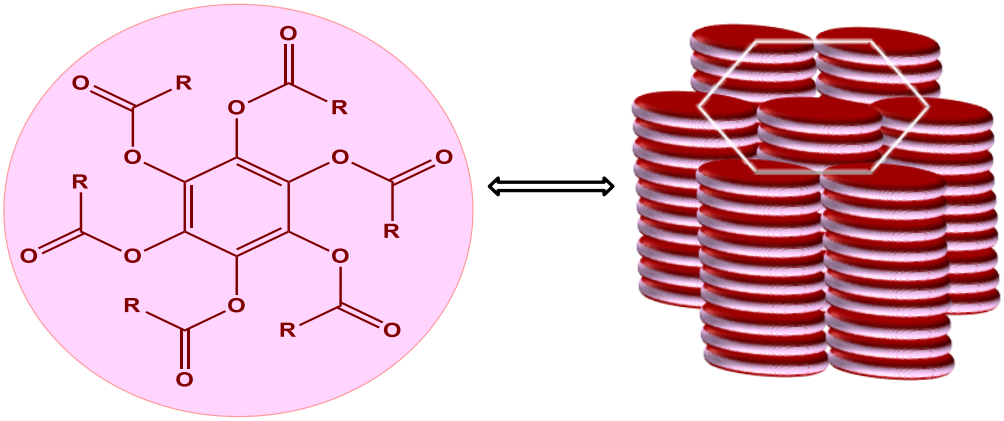

**Figure 6**: Chemical structure of hexa-n-alkanoates of benzene (DLC) and its $Col_h$ phase representation.

Image adapted and redrawn from: Classification and example of LCs by cleanenergywiki

*http://photonicswiki.org/index.php?title=Classification_and_Examples_of_Liquid_Crystals*

- **Banana shaped LCs (BLCs):**

After Calamitics and Discotics, Banana-shaped or Bent shaped LCs are a recent inclusion in the field of LCs. The *IUPAC* defines BLCs as:

*'They are constituted of bent or so-called banana shaped molecules in which two mesogenic groups are linked through a semi-rigid group in such a way as not to be collinear.'*

### 1.2.3.a Bent-core Liquid Crystals

The research in the area of bent-core LCs began in the early 1990s along with the discovery of its unconventional phases and physical properties. In 1996, Niori et al [1] discovered ferroelectric

properties in a new type of mesophase formed by achiral bent-shaped Schiff base derivative (1,3-phenylene bis[4-(4-n-alkoxyphenyliminomethyl)benzoates]) that was synthesized by Matsunaga et al [2]. Figure 7 depicts some of the historic bent-shaped LC molecules with bent-angle 60° and 120° at the central resorcinol core [3].

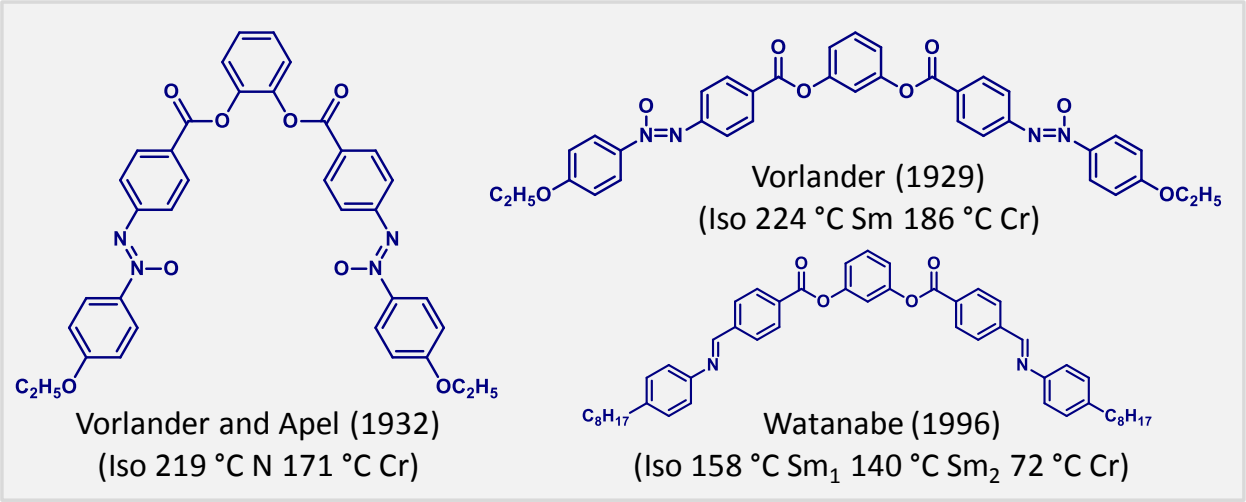


**Figure 7**: Historic bent shaped LCs

Image adapted and redrawn from: *Rev. Mod. Phys.* **2018**, 90, 045004 (1-68)

Bent-core LCs (BLCs) are usually composed of two rod-shaped segments attached to a central angular aromatic core via covalent linkages. The central bend unit governs the bending angle

between two rod-like segments that lead to the bent conformation of the molecule. Bend angle in BLCs ranges from 100-140°. The lateral substitutions (F, Cl, Br, I, $CH_3$, $OCH_3$, CN, etc.) on either central core or outer rings lead to an alteration in overall thermal as well as mesomorphic behavior of the molecule. Some of the central cores explored are Benzene, Naphthalene, Triazole, 1,2,4-Oxadiazole, 1,3,4-Oxadiazole, 1,3-oxazole derivatives, etc [4]. The linkages in the arm segment mainly comprise of -CH=N-, -COO-, -C=C-, etc.

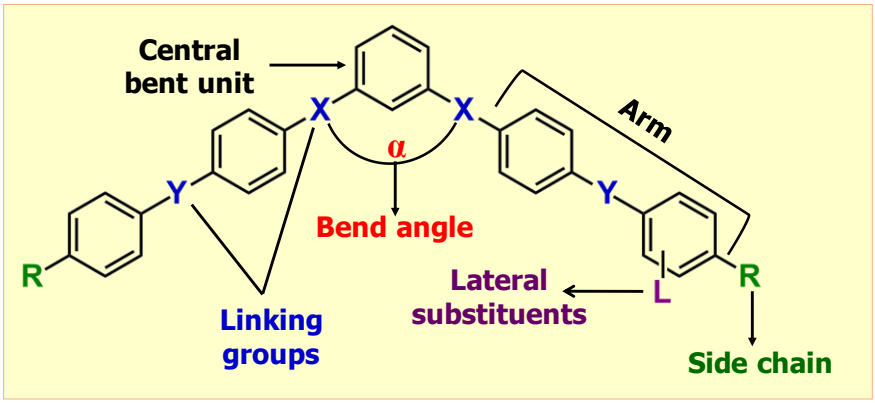


**Figure 8**: A general template for bent-core molecules.

Image adapted and redrawn from: *J. Mater. Chem*, **2007**, 17, 284-298

One of the most interesting property that BLCs possess is the formation of chiral superstructures i.e. possession of chirality in mesophases even when they are achiral. This property arises because BLCs form non-superimposable mirror images due to the alignment of their tilt w.r.t layer normal [5]. Figure 9 explains the formation of non-superimposable microscopic images (under crossed polarizers) for B4 mesophase by uncrossing the analyzer by 5° in the clockwise and anticlockwise direction [6].

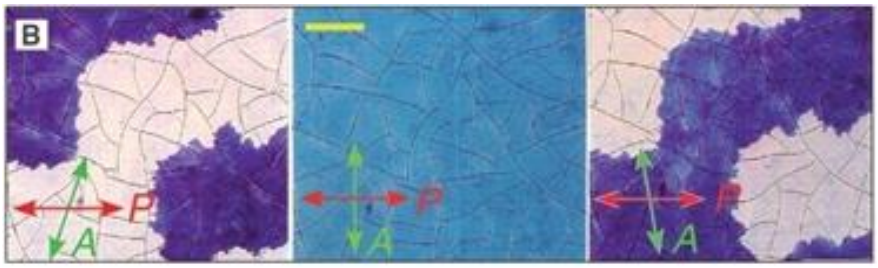


**Figure 9**: Formation of chiral phases [7]

Image adapted and redrawn from: Harden,J.; Chambers, M.; Verduzco, R.; Luchette, P.; Gleeson, J. T.; Sprunt, S.; Jakli, A. Giant flexoelectricity in bent-core nematic liquid crystal elastomers. *App. Phys. Lett*. **2010**, 96, 102907 (1-3).

Molecules having bent-shape are broadly characterized into three types (Figure 10):

**(a) Bent-core mesogens**: Such mesogens have a rigid bent unit, which has two rod-like mesogenic units attached to it. 1,3-disubstituted aromatic rings are the most common type of central core used in the formation of such molecules.

**(b) Bent mesogenic dimers:** This type of molecules is composed of two rod-like mesogenic units attached together by an odd-numbered flexible non-cyclic spacer.

**(c) Hockey-stick molecules:** In such molecules, an alkyl chain is attached to the m-position at one end of the rod-like mesogenic unit.

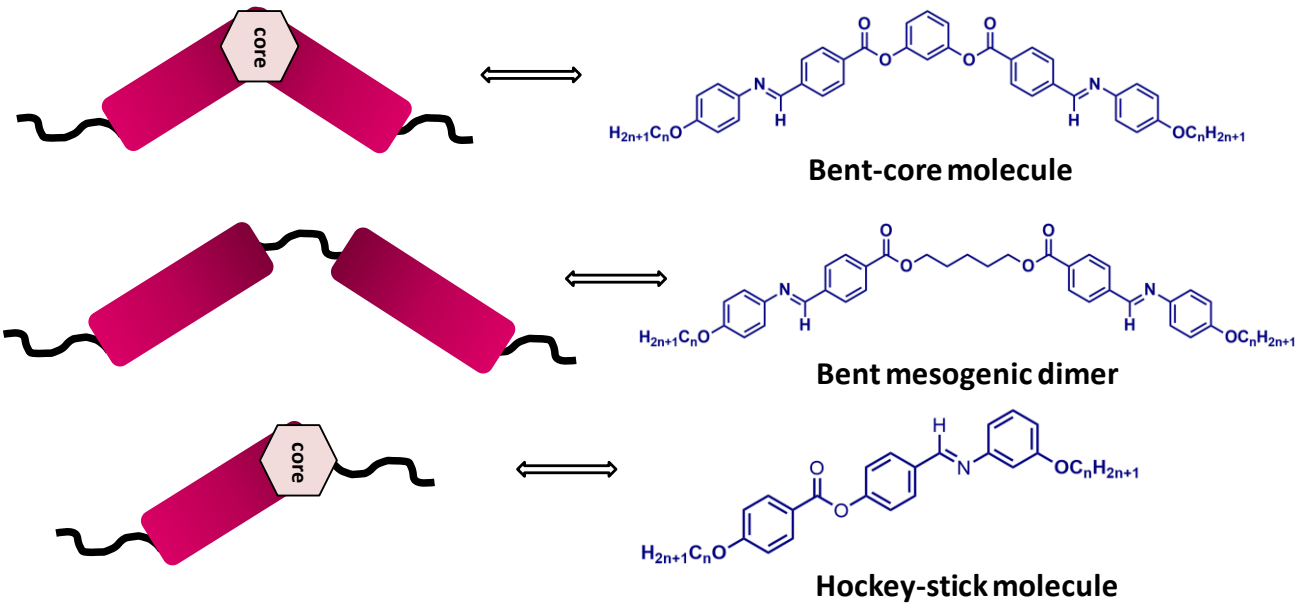


**Figure 10**: Pictorial representation of three types of bent-core molecules.

Image adapted and redrawn from: Amaranatha Reddy, R. A.; Tschierske, C. Bent-core liquid crystals: polar order, superstructural chirality and spontaneous desymmetrisation in soft matter systems. *J. Mater. Chem.* **2006**, 16, 907-961.

### 1.2.3.b Mesophases in BLCs

Origination of nematic and smectic phases along with novel lamellar and columnar phases in BLCs depends upon the bent angle. A typical bent-core molecule favors the formation of Sm phases rather than N due to the presence of kink in molecular shape. The tilted smectic structures (like SmC, $SmCP_A$, etc.) and SmA are most commonly observed smectic phases in BLCs.
The nematic phase in BLCs is favorable due to their unusual properties like giant flexoelectric response [8], chiral domains under electric field [9], etc. but is scarce in the family of BLCs. Therefore, the design of the BLC molecules to induce nematic mesophase is important and depends upon several factors like the bend angle, molecular size, nature of lateral and terminal substituents and linking groups

BLCs also form *banana phases* other than conventional phases (N and Sm) and are categorized as B1-B8 mesophases (where B stands for banana or bent or bow). These phases can be distinguished on the basis of their optical appearance, X-ray diffraction pattern and electro-optical studies.

To study the spectral and structural behavior of a compound, various characterization techniques are used. Moreover, the properties (morphology, thermal behavior, etc.) of a material can also be predicted and examined with the help of different characterization methods. The characterization techniques used are as follows:

For *structural characterization* of the compounds, the instrumentation techniques used were:

- Nuclear Magnetic Resonance (NMR)
- Attenuated Total Reflection (ATR)
- High Resolution Mass Spectrometry (HRMS)
- UV-vis Study

For *material characterization* of the compounds, the instrumentation techniques used were:

- Polarizing Optical Microscopy (POM)
- Differential Scanning Calorimetry (DSC)

# CHAPTER 2

# Synthesis and Characterization of hockey-stick shaped compounds

## 2.1 Introduction

Hockey-stick shaped (unsymmetrical) LCs are classified as a borderline category between symmetric bent-core and calamitic LCs. These unsymmetrical BLCs promote interesting physical properties such as negative bend-splay elastic constants (for the formulation of broad-range blue phases), positive birefringence and dielectric anisotropy. They have relatively low viscosities as compared to rod-like LCs, beneficial for application in electro-optic devices.

Figure 11 describes some unsymmetrical BLCs reported in the literature [10-15]. Nematic, Smectic and B mesophases have been observed in these kinds of BLCs.

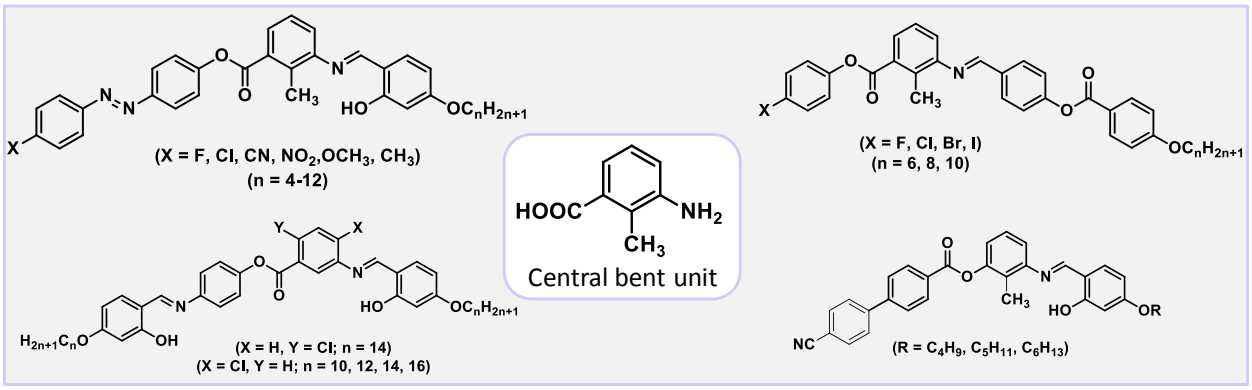


**Figure 11**: Literature reports on four-ring BLCs based on 3-Amino-2-methylbenzoic acid as a central core: ref [10-15].

A hockey-stick shaped molecule has been designed (Figure 12) with the involvement of four phenyl rings where the central core is 3-amino-2-methylbenzoic acid providing the bent molecular architecture. The short arm (polar terminal substituted ring) is tethered to the core by an ester

(-COO-) linkage whereas the long arm is composed of an imine (-CH=N) and an ester linkage with alkyl chains at the end. The imine bond is stabilized by -OH group via the formation of H-bond. The effect of lateral halogen moieties (**X =F, Cl**) at the polar terminal ring of the short arm and the role of the end alkyl chain (**n = 4-18**) at the long arm on the mesomorphic behaviour have been investigated. The polar moieties at the terminal position have been incorporated to enhance the lateral molecular polarizability/dipole moment that would respond as dielectric materials.

* The work has been done in collaboration with Supreet Kaur, PhD, IISER Mohali.

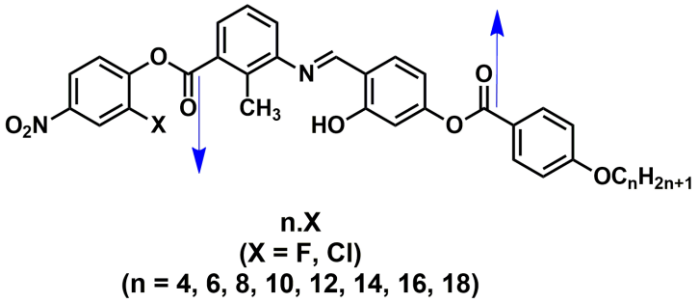


**Figure 12**: Molecular structure of the synthesized compounds.

## 2.2 Results and Discussion

### 2.2.1 Synthesis

Scheme 1 represents the structures of the reactants, intermediates, and products employed to obtain all the final compounds.

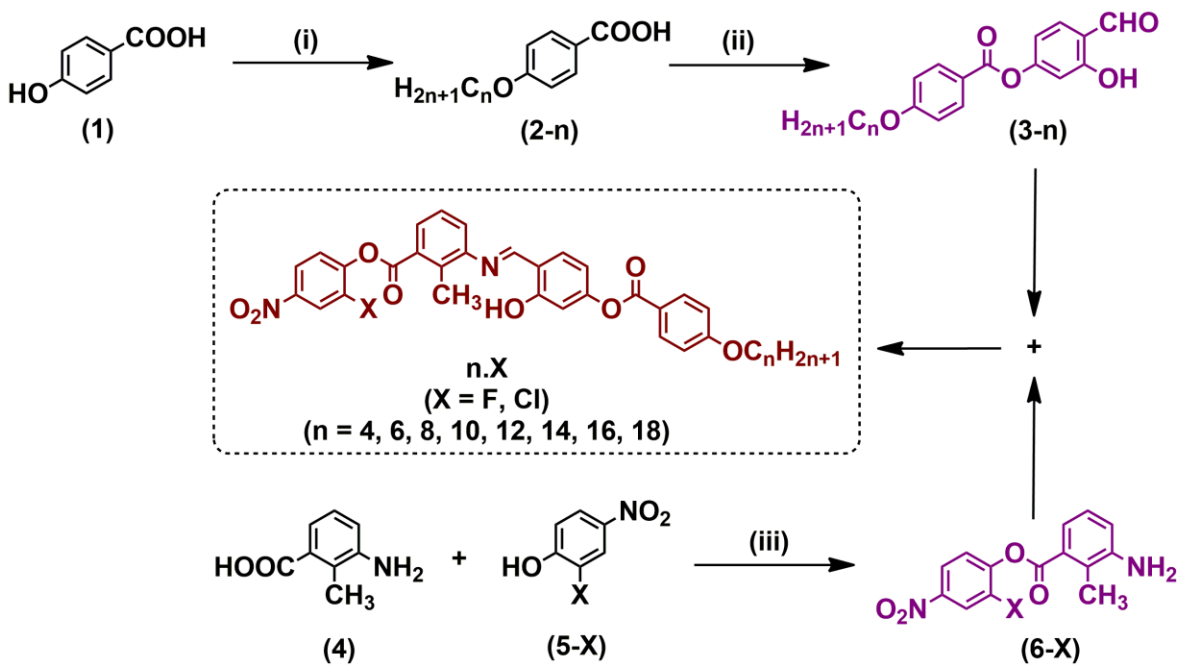


**Scheme 1**: Synthetic details of the compounds: (i) $C_nH_{2n+1}Br$, KOH-EtOH, 6h, KOH-$H_2O$, 3h; (ii) $SOCl_2$, 6h; 2,4-Dihydroxybenzaldehyde, $K_2CO_3$, TBAB, $H_2O$, DCM, 24h; (iii) DCC, DMAP, Dry DCM, 24 h; (iv) Absolute EtOH, glacial AcOH, reflux, 4h.

The procedures described below has been reported earlier in publication: Kaur, S.; Mohiuddin, G.; Satapathy, P.; Nandi, R.; Punjani, V.; Prasad, S. K.; Pal, S. K. Influence of terminal halogen moieties on the phase structure of short-core achiral hockey-stick-shaped mesogens: design, synthesis and structure-property relationship. *Mol. Syst. Des. Eng.* **2018**, 3, 839-852, and we have followed this report for our synthetic procedures.

### 2.2.1.1 Reaction 1: Alkylation

An ethanolic solution of 4-Hydroxybenzoic acid (**1**) was mixed with potassium hydroxide (KOH) (2.5 eq.) solution with further addition of 1-Bromoalkane (1.2 eq.) in refluxing conditions. After 6 hours of stirring,10% KOH was added for base hydrolysis which was then refluxed for 3 more hours. The reaction mixture was then transferred into acid water for neutralization. The white solid (4-(alkoxy)benzoic acid as **2-n**) appeared on constant stirring and was filtered and collected as the product. Yield: 85%

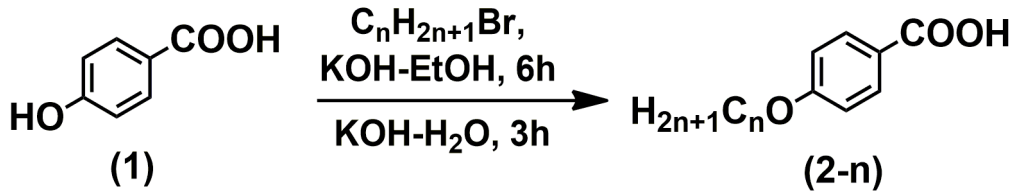


All the homologues with varying the number of carbon atoms (n) in the alkoxy chain (n = 4,6,8,10,12,14,16,18) were synthesized following the procedure in section **2.2.1.1** with suitable amount of Alkyl bromide.

### 2.2.1.2 Reaction 2: Esterification

This procedure has been performed following the report: Nath, R. K.; Deb, R.; Chakraborty, N.; Mohiuddin, G.; Rao, D. S.; Rao, N. V. S.; Influence of chloro substituent on the mesomorphism of unsymmetrical achiral four-ring bent-core compounds. J. Mater. Chem. C, **2013**, 1, 663–670.

4-(alkoxy)benzoic acid (**2-n**) was dissolved in $SOCl_2$ (1.5 mL) to obtain an intermediate 4-(alkoxy)benzoyl chloride under refluxing conditions for 4 hours. In a separate RB flask, 2,4-Dihydroxy benzaldehyde was mixed with water and Potassium carbonate ($K_2CO_3$) (2 eq.) and Tetrabuytlammonium-n-bromide (TBAB) was added to it as a catalyst. To this, (4-(alkoxy)benzoyl chloride) was added along with Dichloromethane (DCM) and was kept on stirring for 24 hours. The extraction of this RM was performed with DCM-water and evaporated to obtain the crude product. This obtained product was purified by column chromatography using silica (100-200 mesh) eluting with a mixture of hexane-ethyl acetate. The ester product obtained was a white solid (**3-n**). Yield: 70 %

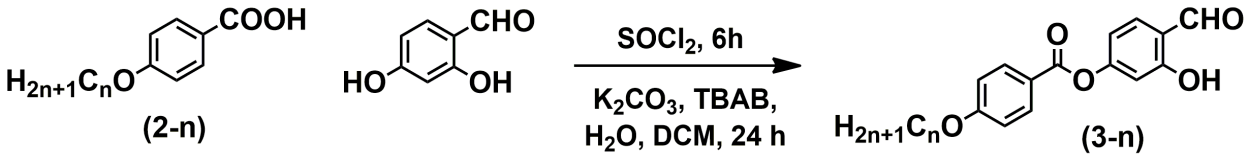


All the ester homologues with varying the number of carbon atoms (n) in the alkoxy chain (n = 4,6,8,10,12,14,16,18) were synthesized following the above procedure.

### 2.2.1.3 Reaction 3: Steglich Esterification

3-Amino-2-methylbenzoic acid (1 eq.) (**4**) was dissolved in dry Dichloromethane (DCM) in an inert nitrogen atmosphere followed by addition of N,N'-Dicyclohexylcarbodiimide (DCC) (1.25 eq.) and 4-Dimethylaminopyridine (DMAP) in a catalytic amount. 2-Halo-4-nitrophenol (1 eq.) (**5-X**) was added to the flask after half an hour of stirring. The RM was then kept on stirring for another 24 hours at RT. The precipitates of Dicyclohexylurea (DCU) were removed by vacuum filtration and the solvent DCM was evaporated to get the solid crude product. The solid product obtained was then recrystallized 2-3 times using absolute ethanol to obtain a pure product which was yellow in color (**6-X**). Yield: 75 %

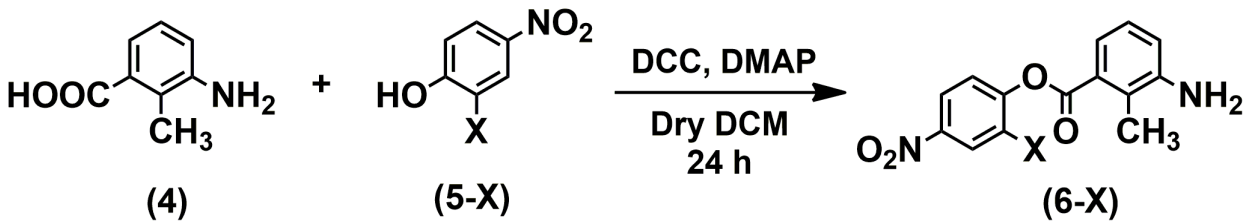


Two compounds were prepared by varying the halogen substitution as X = F, Cl.

### 2.2.1.4 Reaction 4: Schiff's base

The final Schiff base compounds (**n-X**) were prepared by stirring a mixture of ethanolic solution of **6-X** (1 eq.) and **3-n** (1 eq.) for 4 hours under refluxing conditions. To catalyze the reaction, a few drops of glacial acetic acid were added to the RM. The product was obtained in the form of precipitates which was then dissolved in hot boiling ethanol and the insoluble yellow solid was collected as the pure product. Yield: 81 %

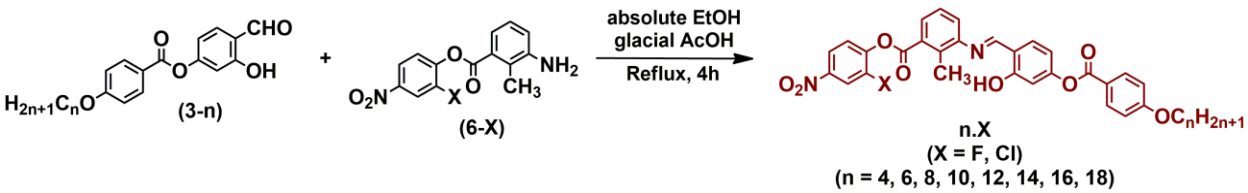


Two series of compounds were prepared (named **n. F** and **n.Cl**) by varying the lateral substitution as X = F, Cl at one end and the alkyl chains (n = 4,6,8,10,12,14,16,18) at the other end.

## 2.2.2 Structural characterization

## Intermediates

Compound **3-4**:

$^{1}$H NMR (400 MHz, $CDCl_3$, $\delta$ in ppm): $\delta$ = 11.25 (s, 1H, -OH), 9.88 (s, 1H, -CHO), 8.12 (d, 2H, *J*= 8.0 Hz, Ar-H), 7.61 (d, 1H, *J*= 8.0 Hz, Ar-H), 6.98 (d, 2H, *J* = 8.0 Hz, Ar-H), 6.91 (d, 1H, *J* = 8.0 Hz, Ar-H), 6.87 (s, 1H, Ar-H), 4.06 (t, 2H, *J* = 6.0 Hz, -$OCH_2$-), 1.85-1.78 (m, 2H, -$CH_2$-), 1.55-1.47 (m, 2H, -$CH_2$-), 1.0 (t, 3H, *J* = 8.0 Hz, -$CH_3$).

$^{13}$C NMR (100 MHz, $CDCl_3$, $\delta$ in ppm): $\delta$ = 13.83, 19.19, 31.10, 68.07, 110.89, 114.19, 114.42, 118.57, 120.68, 132.47, 134.93, 157.89, 163.18, 163.90, 195.50.

ATR ($cm^{-1}$): O-H stretching peak of hydroxyl at 3216 $cm^{-1}$, C-H stretching of alkanes at 2960 $cm^{-1}$, C-H stretching of aldehyde at 2872 $cm^{-1}$, C=O stretching band of ester at 1735 $cm^{-1}$, C=O stretching band of aldehyde at 1728 $cm^{-1}$, C=C (aromatic) stretching band at 1603 $cm^{-1}$, C-O stretching band of ester at 1257 $cm^{-1}$.

UV-vis (nm): 272 nm, 321 nm.

| Compound | M+H | M-H | Exact Mass | Observed Mass | % error |
|---|---|---|---|---|---|
| **3-4** | 315.1232 | 313.1076 | 314.1154 | 313.1063 | 0.00042 |

Compound **3-6**:

$^{1}$H NMR (400 MHz, $CDCl_3$, $\delta$ in ppm): $\delta$ = 11.26 (s, 1H, -OH), 9.89 (s, 1H, -CHO), 8.12 (d, 2H, *J*= 8.0 Hz, Ar-H), 7.61 (d, 1H, *J*= 8.0 Hz, Ar-H), 6.98 (d, 2H, *J* = 8.0 Hz, Ar-H), 6.92 (dd, 1H, *J* = 8.0, 4.0 Hz, Ar-H), 6.88 (d, 1H, *J*= 4.0 Hz Ar-H), 4.05 (t, 2H, *J* = 6.0 Hz, -$OCH_2$-), 1.86-1.79 (m, 2H, -$CH_2$-), 1.52-1.44 (m, 2H, -$CH_2$-), 1.38-1.33 (m, 4H, -$(CH_2)_2$), 0.92 (t, 3H, *J* = 6.0 Hz, -$CH_3$).

$^{13}$C NMR (100 MHz, $CDCl_3$, $\delta$ in ppm): $\delta$ = 14.04, 22.59, 25.65, 29.03, 31.54, 68.40, 110.90, 114.20, 114.43, 118.58, 120.68, 132.48, 134.95, 157.91, 163.20, 163.91, 195.52.

ATR: O-H stretching peak of hydroxyl at 3150 $cm^{-1}$, C-H stretching of alkanes at 2936 $cm^{-1}$, C-H stretching of aldehyde at 2856 $cm^{-1}$, C=O stretching band of aldehyde at 1730 $cm^{-1}$, C=C (aromatic) stretching band at 1603 $cm^{-1}$, C-O stretching band of ester at 1251 $cm^{-1}$.

UV-vis (nm): 271 nm, 322 nm.

| Compound | M+H | M-H | Exact Mass | Observed Mass | % error |
|---|---|---|---|---|---|
| **3-6** | 343.1545 | 341.1389 | 342.1467 | 341.1396 | 0.00020 |

Compound **3-8**:

$^{1}$H NMR (400 MHz, $CDCl_3$, $\delta$ in ppm): $\delta$ = 11.26 (s, 1H, -OH), 9.89 (s, 1H, -CHO), 8.12 (d, 2H, *J*= 8.0 Hz, Ar-H), 7.61 (d, 1H, *J*= 8.0 Hz, Ar-H), 6.98 (d, 2H, *J* = 8.0 Hz, Ar-H), 6.91 (d, 1H, *J* = 8.0 Hz, Ar-H), 6.87 (s, 1H, Ar-H), 4.05 (t, 2H, *J* = 6.0 Hz, -$OCH_2$-), 1.86-1.79 (m, 2H, -$CH_2$-), 1.51-1.44 (m, 2H, -$CH_2$-), 1.38-1.25 (m, 8H, -$(CH_2)_4$), 0.89 (t, 3H, *J* = 8.0 Hz, -$CH_3$).

$^{13}$C NMR (100 MHz, $CDCl_3$, $\delta$ in ppm): $\delta$ = 14.12, 22.66, 25.97, 29.07, 29.22, 29.32, 31.80, 68.40, 110.89, 114.19, 114.42, 118.57, 120.67, 132.47, 134.93, 157.89, 163.18, 163.90, 195.50.

ATR ($cm^{-1}$): O-H stretching peak of hydroxyl at 3161 $cm^{-1}$, C-H stretching of alkanes at 2937 $cm^{-1}$, C-H stretching of aldehyde at 2856 $cm^{-1}$, C=O stretching band of aldehyde at 1728 $cm^{-1}$, C=C (aromatic) stretching band at 1604 $cm^{-1}$, C-O stretching band of ester at 1252 $cm^{-1}$.

UV-vis (nm): 273 nm, 322 nm.

| Compound | M+H | M-H | Exact Mass | Observed Mass | % error |
|---|---|---|---|---|---|
| **3-8** | 371.1858 | 369.1702 | 370.1780 | 369.1718 | 0.00043 |

Compound **3-10**:

$^{1}$H NMR (400 MHz, $CDCl_3$, $\delta$ in ppm): $\delta$ = 11.26 (s, 1H, -OH), 9.88 (s, 1H, -CHO), 8.12 (d, 2H, *J*= 8.0 Hz, Ar-H), 7.61 (d, 1H, *J*= 8.0 Hz, Ar-H), 6.98 (d, 2H, *J* = 12.0 Hz, Ar-H), 6.91 (d, 1H, *J* =

8.0 Hz, Ar-H), 6.88 (s, 1H, Ar-H), 4.05 (t, 2H, *J* = 6.0 Hz, -$OCH_2$-), 1.86-1.79 (m, 2H, -$CH_2$-), 1.51-1.44 (m, 2H, -$CH_2$-), 1.38-1.28 (m, 12H, -$(CH_2)_6$), 0.88 (t, 3H, *J* = 6.0 Hz, -$CH_3$).

$^{13}$C NMR (100 MHz, $CDCl_3$, $\delta$ in ppm): $\delta$ = 14.13, 22.69, 25.97, 29.06, 29.32, 29.36, 29.55 31.90, 68.40, 110.89, 114.19, 114.42, 118.57, 120.67, 132.47, 134.93, 157.89, 163.18, 163.90, 195.50.

ATR ($cm^{-1}$): O-H stretching peak of hydroxyl at 3115 $cm^{-1}$, C-H stretching of alkanes at 2917 $cm^{-1}$, C-H stretching of aldehyde at 2850 $cm^{-1}$, C=O stretching band of aldehyde at 1730 $cm^{-1}$, C=C (aromatic) stretching band at 1603 $cm^{-1}$, C-O stretching band of ester at 1254 $cm^{-1}$.

UV-vis (nm): 273 nm, 321 nm.

| **Compound** | **M+H** | **M-H** | **Exact Mass** | **Observed Mass** | **% error** |
|---|---|---|---|---|---|
| **3-10** | 399.2171 | 397.2015 | 398.2093 | 397.2029 | 0.00035 |

Compound **3-12**:

$^{1}$H NMR (400 MHz, $CDCl_3$, $\delta$ in ppm): $\delta$ = 11.26 (s, 1H, -OH), 9.88 (s, 1H, -CHO), 8.12 (d, 2H, *J*= 8.0 Hz, Ar-H), 7.61 (d, 1H, *J* = 8.0 Hz, Ar-H), 6.98 (d, 2H, *J* = 12.0 Hz, Ar-H), 6.91 (d, 1H, *J* = 8.0 Hz, Ar-H), 6.88 (s, 1H, Ar-H), 4.05 (t, 2H, *J* = 8.0 Hz, -$OCH_2$-), 1.86-1.79 (m, 2H, -$CH_2$-),

1.51-1.44 (m, 2H, -$CH_2$-), 1.38-1.27 (m, 16H, -$(CH_2)_8$), 0.88 (t, 3H, *J* = 6.0 Hz, -$CH_3$).

$^{13}$C NMR (100 MHz, $CDCl_3$, $\delta$ in ppm): $\delta$ = 14.14, 22.70, 25.97, 29.06, 29.36, 29.56, 29.59, 29.64, 29.66, 31.92, 68.39, 110.89, 114.19, 114.42, 118.57, 120.66, 132.46, 134.93, 157.89, 163.18, 163.90, 195.50.

ATR ($cm^{-1}$): O-H stretching peak of hydroxyl at 3228 $cm^{-1}$, C-H stretching of alkanes at 2916 $cm^{-1}$, C-H stretching of aldehyde at 2854 $cm^{-1}$, C=O stretching band of aldehyde at 1728 $cm^{-1}$, C=C (aromatic) stretching band at 1604 $cm^{-1}$, C-O stretching band of ester at 1252 $cm^{-1}$.

UV-vis (nm): 273 nm, 322 nm.

| **Compound** | **M+H** | **M-H** | **Exact Mass** | **Observed Mass** | **% error** |
|---|---|---|---|---|---|

| | | | | | |
|---|---|---|---|---|---|
| **3-12** | 427.2484 | 425.2328 | 426.2406 | 425.2346 | 0.00042 |

Compound **3-14**:

$^{1}$H NMR (400 MHz, $CDCl_3$, $\delta$ in ppm): $\delta$ = 11.26 (s, 1H, -OH), 9.88 (s, 1H, -CHO), 8.12 (d, 2H, *J*= 8.0 Hz, Ar-H), 7.61 (d, 1H, *J*= 8.0 Hz, Ar-H), 6.98 (d, 2H, *J* = 12.0 Hz, Ar-H), 6.91 (d, 1H, *J* = 8.0 Hz, Ar-H), 6.88 (s, 1H, Ar-H), 4.04 (t, 2H, *J* = 6.0 Hz, -$OCH_2$-), 1.86-1.79 (m, 2H, -$CH_2$-), 1.51-1.44 (m, 2H, -$CH_2$-), 1.38-1.26 (m, 20H, -$(CH_2)_{10}$), 0.88 (t, 3H, *J* = 8.0 Hz, -$CH_3$).

$^{13}$C NMR (100 MHz, $CDCl_3$, $\delta$ in ppm): $\delta$ = 14.14, 22.70, 25.97, 29.07, 29.37, 29.56, 29.59, 29.66, 29.68, 29.70, 31.93, 68.40, 110.89, 114.19, 114.42, 118.57, 120.67, 132.47, 134.93, 157.90, 163.19, 163.90, 195.50.

ATR ($cm^{-1}$): O-H stretching peak of hydroxyl at 3229 $cm^{-1}$, C-H stretching of alkanes at 2916 $cm^{-1}$, C-H stretching of aldehyde at 2850 $cm^{-1}$, C=O stretching band of aldehyde at 1728 $cm^{-1}$, C=C (aromatic) stretching band at 1604 $cm^{-1}$, C-O stretching band of ester at 1252 $cm^{-1}$.

UV-vis (nm): 272 nm, 322 nm.

| **Compound** | **M+H** | **M-H** | **Exact Mass** | **Observed Mass** | **% error** |
|---|---|---|---|---|---|
| **3-14** | 455.2797 | 453.2641 | 454.2719 | 453.2632 | 0.00019 |

Compound **3-16**:

$^{1}$H NMR (400 MHz, $CDCl_3$, $\delta$ in ppm): $\delta$ = 11.25 (s, 1H, -OH), 9.88 (s, 1H, -CHO), 8.12 (d, 2H, *J*= 8.0 Hz, Ar-H), 7.61 (d, 1H, *J*= 8.0 Hz, Ar-H), 6.97 (d, 2H, *J* = 8.0 Hz, Ar-H), 6.91 (d, 1H, *J* = 8.0 Hz, Ar-H), 6.87 (s, 1H, Ar-H), 4.05 (t, 2H, *J* = 8.0 Hz, -$OCH_2$-), 1.85-1.79 (m, 2H, -$CH_2$-), 1.51-1.44 (m, 2H, -$CH_2$-), 1.38-1.26 (m, 24H, -$(CH_2)_{12}$), 0.88 (t, 3H, *J* = 6.0 Hz, -$CH_3$).

$^{13}$C NMR (100 MHz, $CDCl_3$, $\delta$ in ppm): $\delta$ = 14.14, 22.70, 25.97, 29.07, 29.37, 29.56, 29.59, 29.67, 29.70, 31.93, 68.40, 110.89, 114.18, 114.43, 118.58, 120.68, 132.47, 134.93, 157.90, 163.19, 163.90, 195.49.

ATR ($cm^{-1}$): O-H stretching peak of hydroxyl at 3228 $cm^{-1}$, C-H stretching of alkanes at 2916 $cm^{-1}$, C-H stretching of aldehyde at 2848 $cm^{-1}$, C=O stretching band of aldehyde at 1728 $cm^{-1}$, C=C (aromatic) stretching band at 1604 $cm^{-1}$, C-O stretching band of ester at 1252 $cm^{-1}$.

UV-vis (nm): 273 nm, 322 nm.

| Compound | M+H | M-H | Exact Mass | Observed Mass | % error |
|---|---|---|---|---|---|
| **3-16** | 483.3110 | 481.2954 | 482.3032 | 481.2973 | 0.00039 |

Compound **3-18**:

$^{1}$H NMR (400 MHz, $CDCl_3$, $\delta$ in ppm): $\delta$ = 11.25 (s, 1H, -OH), 9.88 (s, 1H, -CHO), 8.12 (d, 2H, *J*= 8.0 Hz, Ar-H), 7.61 (d, 1H, *J*= 8.0 Hz, Ar-H), 6.98 (d, 2H, *J* = 8.0 Hz, Ar-H), 6.91 (d, 1H, *J* = 8.0 Hz, Ar-H), 6.88 (s, 1H, Ar-H), 4.05 (t, 2H, *J* = 8.0 Hz, -$OCH_2$-), 1.86-1.79 (m, 2H, -$CH_2$-), 1.51-1.44 (m, 2H, -$CH_2$-), 1.38-1.26 (m, 28H, -$(CH_2)_{14}$), 0.88 (t, 3H, *J* = 6.0 Hz, -$CH_3$).

$^{13}$C NMR (100 MHz, $CDCl_3$, $\delta$ in ppm): $\delta$ = 14.14, 22.70, 25.97, 29.07, 29.37, 29.56, 29.60, 29.67, 29.71, 31.93, 68.40, 110.89, 114.18, 114.42, 118.57, 120.67, 132.47, 134.93, 157.90, 163.18, 163.90, 195.50.

ATR ($cm^{-1}$): O-H stretching peak of hydroxyl at 3230 $cm^{-1}$, C-H stretching of alkanes at 2914 $cm^{-1}$, C-H stretching of aldehyde at 2848 $cm^{-1}$, C=O stretching band of aldehyde at 1732 $cm^{-1}$, C=C (aromatic) stretching band at 1608 $cm^{-1}$, C-O stretching band of ester at 1255 $cm^{-1}$.

UV-vis (nm): 273 nm, 321 nm

| Compound | M+H | M-H | Exact Mass | Observed Mass | % error |
|---|---|---|---|---|---|
| **3-18** | 511.3423 | 509.3267 | 510.3345 | 509.3247 | 0.00039 |

Compound **6-F**:

$^{1}$H NMR (400 MHz, $CDCl_3$, $\delta$ in ppm): $\delta$ = 8.14-8.11 (m, 2H, Ar-H) 7.54 (d, 1H, *J*= 8.0 Hz, Ar-

H), 7.47 (t, 1H, *J* = 8.0 Hz, Ar-H), 7.16 (t, 1H, *J* = 8.0 Hz, Ar-H), 6.94 (d, 1H, *J*= 8.0 Hz, Ar-H), 3.83 (s, 2H, -$NH_2$), 2.43 (s, 3H, -$CH_3$).

$^{13}$C NMR (100 MHz, $CDCl_3$, $\delta$ in ppm): $\delta$= 13.85, 112.84, 113.08, 119.79, 120.14, 120.18, 121.42, 124.56, 124.65, 126.39, 128.24, 143.98, 144.11, 145.67, 145.75, 145.91, 152.57, 155.11, 164.47.

ATR ($cm^{-1}$): N-H stretching peak of aromatic amine at 3358 $cm^{-1}$, C=O stretching band of ester at 1737 $cm^{-1}$, N-O stretching band of nitro at 1517 $cm^{-1}$, C-N stretching band at 1249 $cm^{-1}$, C-F stretching band at 1188 $cm^{-1}$.

UV-vis (nm): 267 nm.

| **Compound** | **M+H** | **M-H** | **Exact Mass** | **Observed Mass** | **% error** |
|---|---|---|---|---|---|
| **6-F** | 291.0781 | 289.0625 | 290.0703 | 291.0770 | 0.00038 |

Compound **6-Cl**:

$^{1}$H NMR (400 MHz, $CDCl_3$, $\delta$ in ppm): $\delta$ = 8.41 (s, 1H, Ar-H), 8.24 (d, 1H, *J* = 12.0, Ar-H) 7.63 (d, 1H, *J*= 8.0 Hz, Ar-H), 7.48 (d, 1H, *J* = 12.0 Hz, Ar-H), 7.18 (t, 1H, *J* = 8.0 Hz, Ar-H), 6.96 (d, 1H, *J*= 6.0 Hz Ar-H), 3.83 (s, 2H, -$NH_2$), 2.45 (s, 3H, -$CH_3$).

$^{13}$C NMR (100 MHz, $CDCl_3$, $\delta$ in ppm): $\delta$= 13.84, 112.84, 113.08, 119.79, 120.14, 120.18, 121.42, 124.56, 124.65, 126.39, 128.24, 143.98, 144.11, 145.67, 145.75, 145.91, 152.57, 155.11, 164.47.

ATR ($cm^{-1}$): N-H stretching peak of aromatic amine at 3341 $cm^{-1}$, C=O stretching band of ester at 1741 $cm^{-1}$, N-O stretching band of nitro at 1522 $cm^{-1}$, C-N stretching band at 1223 $cm^{-1}$, C-Cl stretching band at 742 $cm^{-1}$.

UV-vis (nm): 265 nm.

| **Compound** | **M+H** | **M-H** | **Exact Mass** | **Observed Mass** | **% error** |
|---|---|---|---|---|---|
| **6-Cl** | 307.0485 | 305.0329 | 306.0407 | 307.0500 | 0.00048 |

# Final compounds

Compound **4.F**:

$^{1}$H NMR (400 MHz, $CDCl_3$, $\delta$ in ppm): $\delta$ = 13.25 (s, 1H, -OH), 8.55 (s, 1H, -CH=N-), 8.14 (d, 4H, *J* = 8.0 Hz, Ar-H), 8.06 (d, 1H, *J* = 8.0 Hz, Ar-H), 7.53-7.41 (m, 3H, Ar-H), 7.32 (d, 1H, *J* = 8.0 Hz, Ar-H), 6.98 (d, 2H, *J* = 8.0 Hz, Ar-H), 6.92 (s, 1H, Ar-H), 6.87 (d, 1H, *J* = 8.0 Hz, Ar-H), 4.06 (t, 2H, *J* = 6.0 Hz, -$OCH_2$-), 2.68 (s, 3H, -$CH_3$), 1.85-1.78 (m, 2H, -$CH_2$), 1.57-1.48 (m,2H, -$CH_2$), 1.00 (t, 3H, *J* = 8.0 Hz, -$CH_3$). (Figure 13)

$^{13}$C NMR (100 MHz, $CDCl_3$, $\delta$ in ppm):$\delta$= 13.84, 15.47, 19.20, 31.11, 68.05, 110.77, 112.91, 113.15, 113.46, 114.36, 117.01, 120.20, 120.24, 121.03, 123.58, 124.62, 126.89, 128.66, 129.26, 132.41, 133.43, 135.16, 143.75, 143.88, 145.89, 149.56, 152.51, 155.05, 155.33, 162.51, 163.32, 163.65, 163.75, 164.34. (figure 14)

ATR ($cm^{-1}$): C-H stretching of alkanes at 2942 $cm^{-1}$, O-H (intramolecular) stretching peak of hydroxyl at 3102 $cm^{-1}$, C=O stretching band of ester at 1753, 1718 $cm^{-1}$, HC=N stretching of an imine at 1623 $cm^{-1}$, C=C (aromatic) stretching band at 1608 $cm^{-1}$, N-O stretching band of nitro at 1528 $cm^{-1}$,C-F stretching band at 1256 $cm^{-1}$.

UV-vis (nm): 276 nm, 337 nm.

| Compound | M+H | M-H | Exact Mass | Observed Mass | % error |
|---|---|---|---|---|---|
| **4.F** | 587.1829 | 585.1673 | 586.1751 | 587.1858 | 0.00049 |

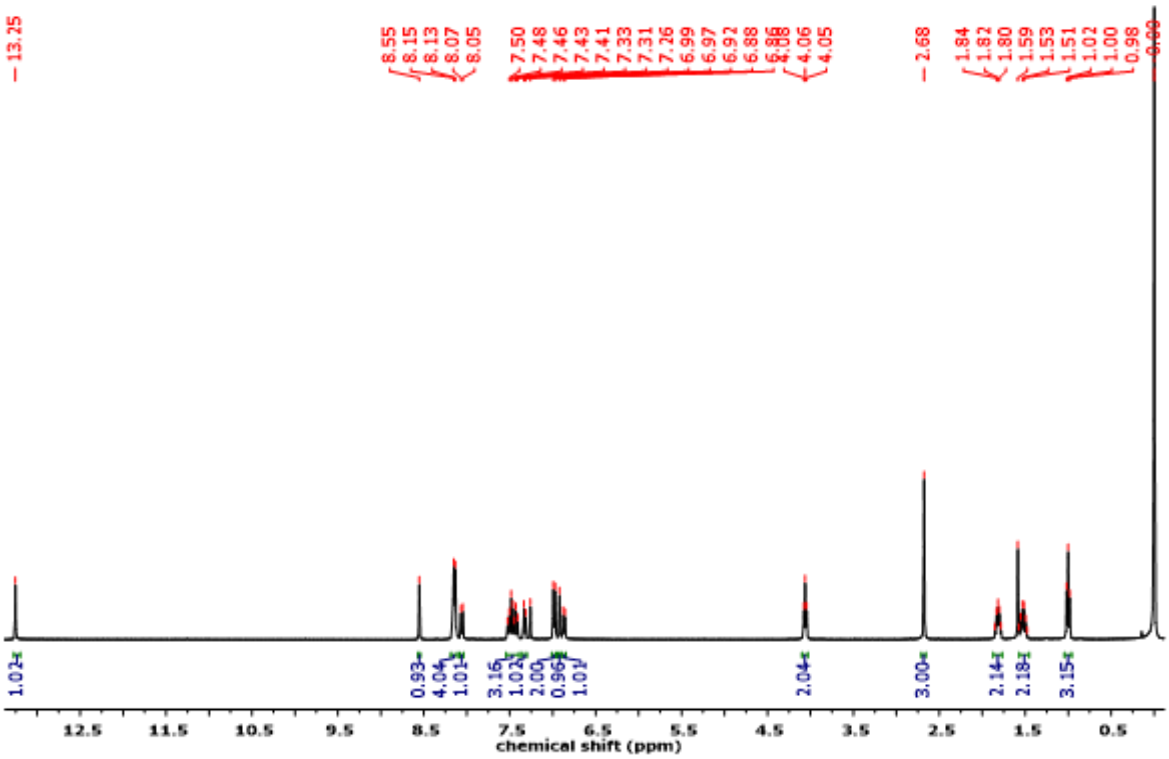


**Figure 13**: $^{1}$H NMR of compound **4.F**.

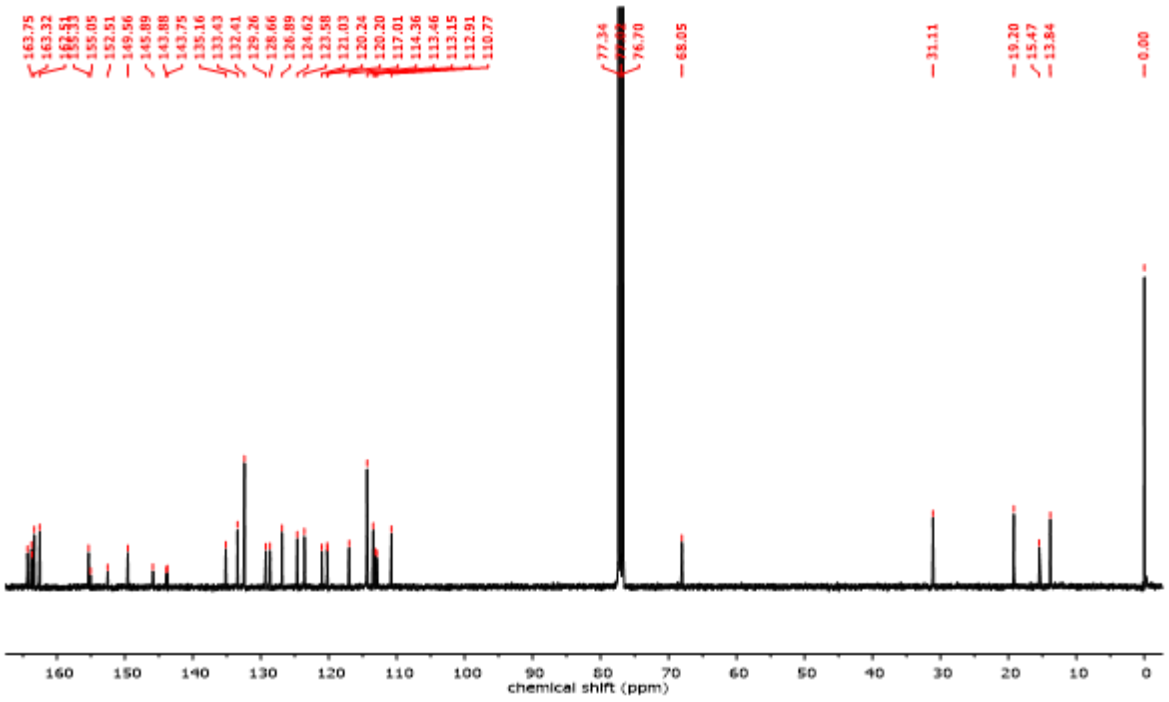


**Figure 14**: $^{13}$C NMR of compound **4.F**.

Compound **6.F**:

$^{1}$H NMR (400 MHz, $CDCl_3$, $\delta$ in ppm): $\delta$ = 13.25 (s, 1H, -OH), 8.55 (s, 1H, -CH=N-), 8.14 (d, 4H, *J* = 8.0 Hz, Ar-H), 8.06 (d, 1H, *J* = 8.0 Hz, Ar-H), 7.53-7.41 (m, 3H, Ar-H), 7.33 (d, 1H, *J* = 8.0 Hz, Ar-H), 6.98 (d, 2H, *J* = 8.0 Hz, Ar-H), 6.92 (s, 1H, Ar-H), 6.87 (d, 1H, *J* = 8.0 Hz, Ar-H), 4.05 (t, 2H, *J* = 6.0 Hz, -$OCH_2$-), 2.68 (s, 3H, -$CH_3$), 1.86-1.79 (m, 2H, -$CH_2$), 1.52-1.45 (m, 2H, -$CH_2$-), 1.36 (d, 4H, *J* = 3.32 Hz –$(CH_2)_2$-), 0.92 (t, 3H, *J* = 6.0 Hz, -$CH_3$).

$^{13}$C NMR (100 MHz, $CDCl_3$, $\delta$ in ppm): $\delta$= 14.04, 15.47, 22.60, 25.66, 29.05, 31.55, 68.37, 110.77, 112.92, 113.16, 113.46, 114.36, 117.01, 120.20, 120.24, 121.02, 123.58, 124.62, 126.89, 128.66, 129.26, 132.41, 133.43, 135.16, 143.75, 143.88, 145.90, 149.58, 152.52, 155.05, 155.33, 162.51, 163.32, 163.65, 163.75, 164.34.

ATR ($cm^{-1}$): C-H stretching of alkanes at 2937 $cm^{-1}$, O-H (intramolecular) stretching peak of hydroxyl at 3108 $cm^{-1}$, C=O stretching band of ester at 1760, 1719 $cm^{-1}$, HC=N stretching of an imine at 1622 $cm^{-1}$, C=C (aromatic) stretching band at 1608 $cm^{-1}$, N-O stretching band of nitro at 1531 $cm^{-1}$, C-F stretching band at 1257 $cm^{-1}$.

UV-vis (nm): 277 nm, 336 nm.

| **Compound** | **M+H** | **M-H** | **Exact Mass** | **Observed Mass** | **% error** |
|---|---|---|---|---|---|
| **6.F** | 615.2142 | 613.1986 | 614.2064 | 615.2164 | 0.00036 |

Compound **8.F**:

$^{1}$H NMR (400 MHz, $CDCl_3$, $\delta$ in ppm): $\delta$ = 13.25 (s, 1H, -OH), 8.56 (s, 1H, -CH=N-), 8.17-8.14 (m, 4H, Ar-H), 8.06 (d, 1H, *J* = 8.0 Hz, Ar-H), 7.53-7.41 (m, 3H, Ar-H), 7.33 (d, 1H, *J* = 8.0 Hz, Ar-H), 6.98 (d, 2H, *J* = 8.0 Hz, Ar-H), 6.92 (s, 1H, Ar-H), 6.87 (d, 1H, *J* = 8.0 Hz, Ar-H), 4.05 (t, 2H, *J* = 8.0 Hz, -$OCH_2$-), 2.68 (s, 3H, -$CH_3$), 1.86-1.79 (m, 2H, -$CH_2$-), 1.52-1.45 (m, 2H, -$CH_2$-), 1.39-1.26 (m, 20H, -$(CH_2)_4$-), 0.90 (t, 3H, *J* = 6.0 Hz, -$CH_3$).

$^{13}$C NMR (100 MHz, $CDCl_3$, $\delta$ in ppm): $\delta$= 14.12, 15.48, 22.67, 25.99, 29.09, 29.23, 29.33, 31.81, 69.39, 110.79, 112.94, 113.48, 114.38, 117.03, 120.25, 121.06, 123.59, 124.62, 126.90, 128.69,

129.28, 132.43, 133.44, 135.17, 143.77, 144.83, 149.62, 155.37, 162.54, 163.34, 163.67, 163.78, 164.36.

ATR ($cm^{-1}$): C-H stretching of alkanes at 2918 $cm^{-1}$, O-H (intramolecular) stretching peak of hydroxyl at 3104 $cm^{-1}$, C=O stretching band of ester at 1751, 1719 $cm^{-1}$, HC=N stretching of an imine at 1621 $cm^{-1}$, C=C (aromatic) stretching band at 1610 $cm^{-1}$, N-O stretching band of nitro at 1527 $cm^{-1}$, C-F stretching band is at 1255 $cm^{-1}$.

UV-vis (nm): 276 nm, 337 nm.

| **Compound** | **M+H** | **M-H** | **Exact Mass** | **Observed Mass** | **% error** |
|---|---|---|---|---|---|
| **8.F** | 643.2455 | 641.2299 | 642.2377 | 643.2477 | 0.00034 |

Compound **10.F**:

$^{1}H$ NMR (400 MHz, $CDCl_3$, $\delta$ in ppm): $\delta$ = 13.25 (s, 1H, -OH), 8.56 (s, 1H, -CH=N-), 8.17-8.13 (m, 4H, Ar-H), 8.06 (d, 1H, *J* = 8.0 Hz, Ar-H), 7.53-7.41 (m, 3H, Ar-H), 7.33 (d, 1H, *J* = 8.0 Hz, Ar-H), 6.98 (d, 2H, *J* = 8.0 Hz, Ar-H), 6.92 (s, 1H, Ar-H), 6.87 (d, 1H, *J* = 8.0 Hz, Ar-H), 4.05 (t, 2H, *J* = 8.0 Hz, -$OCH_2$-), 2.68 (s, 3H, -$CH_3$), 1.86-1.79 (m, 2H, -$CH_2$-), 1.51-1.44 (m, 2H, -$CH_2$), 1.38-1.28 (m, 12H, -$(CH_2)_6$-), 0.89 (t, 3H, *J* = 6.0 Hz, -$CH_3$).

$^{13}C$ NMR (100 MHz, $CDCl_3$, $\delta$ in ppm): $\delta$= 14.14, 15.48, 22.69, 25.98, 29.08, 29.33, 29.37, 29.56, 31.90, 69.38, 110.78, 112.93, 113.17, 113.47, 114.37, 117.02, 120.21, 120.25, 121.03, 123.59, 124.63, 126.90, 128.67, 129.27, 132.42, 133.44, 135.17, 143.76 145.91, 149.59, 152.53, 155.34, 162.53, 163.34, 163.66, 163.77, 164.36.

ATR ($cm^{-1}$): C-H stretching of alkanes at 2917 $cm^{-1}$, O-H (intramolecular) stretching peak of hydroxyl at 3107 $cm^{-1}$, C=O stretching band of ester at 1757, 1720 $cm^{-1}$, HC=N stretching of an imine at 1621 $cm^{-1}$, C=C (aromatic) stretching band at 1605 $cm^{-1}$, N-O stretching band of nitro at 1526 $cm^{-1}$, C-F stretching band is at 1258 $cm^{-1}$.

UV-vis (nm): 276 nm, 336 nm.

| Compound | M+H | M-H | Exact Mass | Observed Mass | % error |
|---|---|---|---|---|---|
| **10.F** | 671.2768 | 669.2612 | 670.2690 | 671.2780 | 0.00018 |

Compound **12.F**:

$^{1}$H NMR (400 MHz, $CDCl_3$, $\delta$ in ppm): $\delta$ = 13.26 (s, 1H, -OH), 8.55 (s, 1H, -CH=N-), 8.14 (d, 4H, *J* = 8.0 Hz, Ar-H), 8.06 (d, 1H, *J* = 8.0 Hz, Ar-H), 7.53-7.41 (m, 3H, Ar-H), 7.33 (d, 1H, *J* = 8.0 Hz, Ar-H), 6.98 (d, 2H, *J* = 8.0 Hz, Ar-H), 6.92 (s, 1H, Ar-H), 6.87 (d, 1H, *J* = 8.0 Hz, Ar-H), 4.05 (t, 2H, *J* = 8.0 Hz, -$OCH_2$-), 2.68 (s, 3H, -$CH_3$), 1.86-1.79 (m, 2H, -$CH_2$), 1.51-1.44 (m, 2H, -$CH_2$), 1.38-1.27 (m, 16H, -$(CH_2)_8$-), 0.89 (t, 3H, *J* = 6.0 Hz, -$CH_3$).

$^{13}$C NMR (100 MHz, $CDCl_3$, $\delta$ in ppm): $\delta$= 14.14, 15.46, 22.70, 25.98, 29.08, 29.57, 29.60, 29.64, 29.66, 31.92, 69.37, 110.76, 112.90, 113.14, 113.45, 114.36, 117.00, 120.23, 121.01, 123.57, 124.61, 126.89, 128.64, 129.26, 132.40, 133.43, 135.16, 143.74, 143.87, 145.88, 149.55, 152.51, 155.04, 155.32, 162.50, 163.31, 163.64, 163.75, 164.33.

ATR ($cm^{-1}$): C-H stretching of alkanes at 2916 $cm^{-1}$, O-H (intramolecular) stretching peak of hydroxyl at 3108 $cm^{-1}$, C=O stretching band of ester at 1752, 1721 $cm^{-1}$, HC=N stretching of an imine at 1621 $cm^{-1}$, C=C (aromatic) stretching band at 1603$cm^{-1}$, N-O stretching band of nitro at 1530 $cm^{-1}$, C-F stretching band is at 1254 $cm^{-1}$.

UV-vis (nm): 276 nm, 337 nm.

| Compound | M+H | M-H | Exact Mass | Observed Mass | % error |
|---|---|---|---|---|---|
| **12.F** | 699.3081 | 697.2925 | 698.3003 | 699.3114 | 0.00047 |

Compound **14.F**:

$^{1}$H NMR (400 MHz, $CDCl_3$, $\delta$ in ppm): $\delta$ = 13.25 (s, 1H, -OH), 8.55 (s, 1H, -CH=N-), 8.17-8.13 (m, 4H, Ar-H), 8.06 (d, 1H, *J* = 8.0 Hz, Ar-H), 7.53-7.41 (m, 3H, Ar-H), 7.33 (d, 1H, *J* = 8.0 Hz,

Ar-H), 6.98 (d, 2H, *J* = 8.0 Hz, Ar-H), 6.92 (s, 1H, Ar-H), 6.87 (d, 1H, *J* = 8.0 Hz, Ar-H), 4.05 (t, 2H, *J* = 8.0 Hz, -$OCH_2$-), 2.68 (s, 3H, -$CH_3$), 1.86-1.79 (m, 2H, -$CH_2$-), 1.56-1.44 (m, 2H, -$CH_2$), 1.36-1.26 (m, 20H, -$(CH_2)_{10}$-), 0.88 (t, 3H, *J* = 8.0 Hz, -$CH_3$).

$^{13}$C NMR (100 MHz, $CDCl_3$, $\delta$ in ppm): $\delta$= 14.14, 15.47, 22.70, 25.98, 29.09, 29.37, 29.56, 29.60, 29.66, 29.68, 29.70, 31.93, 69.38, 110.78, 112.93, 113.16, 113.47, 114.37, 117.01, 120.21, 121.03, 123.59, 124.62, 126.89, 128.67, 129.27, 132.41, 133.43, 135.16, 143.75, 149.59, 152.52, 155.06, 155.34, 162.52, 163.33, 163.66, 163.76, 164.34.

ATR ($cm^{-1}$): HC=N stretching of an imine at 1621 $cm^{-1}$, C=O stretching band of ester at 1750, 1723 $cm^{-1}$, C-H stretching of alkanes at 2915 $cm^{-1}$, O-H (intramolecular) stretching peak of hydroxyl at 3101 $cm^{-1}$, C=C (aromatic) stretching band at 1602 $cm^{-1}$, N-O stretching band of nitro at 1527 $cm^{-1}$, C-F stretching band is at 1257 $cm^{-1}$.

UV-vis (nm): 276 nm, 337 nm.

| **Compound** | **M+H** | **M-H** | **Exact Mass** | **Observed Mass** | **% error** |
|---|---|---|---|---|---|
| **14.F** | 727.3394 | 725.3238 | 726.3316 | 727.3426 | 0.00044 |

Compound **16.F**:

$^{1}$H NMR (400 MHz, $CDCl_3$, $\delta$ in ppm): $\delta$ = 13.26 (s, 1H, -OH), 8.55 (s, 1H, -CH=N-), 8.16-8.13 (m, 4H, Ar-H), 8.06 (d, 1H, *J* = 8.0 Hz, Ar-H), 7.53-7.41 (m, 3H, Ar-H), 7.33 (d, 1H, *J* = 8.0 Hz, Ar-H), 6.98 (d, 2H, *J* = 8.0 Hz, Ar-H), 6.92 (s, 1H, Ar-H), 6.87 (d, 1H, *J* = 8.0 Hz, Ar-H), 4.05 (t,

2H, *J* = 8.0 Hz, -$OCH_2$-), 2.68 (s, 3H, -$CH_3$), 1.86-1.79 (m, 2H, -$CH_2$-), 1.51-1.44 (m, 2H, -$CH_2$), 1.36-1.26 (m, 24H, -$(CH_2)_{12}$-), 0.88 (t, 3H, *J* = 8.0 Hz, -$CH_3$).

$^{13}$C NMR (100 MHz, $CDCl_3$, $\delta$ in ppm): $\delta$ = 14.15, 15.47, 22.71, 25.98, 25.98, 29.09, 29.38, 29.57, 29.60, 29.67, 29.71, 31.94, 68.38, 110.78, 112.92, 113.16, 113.47, 114.37, 117.02, 120.21, 120.25, 121.02, 123.59, 124.62, 126.90, 128.66, 129.28, 132.42, 133.44, 135.17, 143.76, 143.89, 145.90, 149.58, 152.52, 155.06, 155.34, 162.52, 163.33, 163.66, 163.76, 164.35

ATR ($cm^{-1}$): HC=N stretching of an imine at 1618 $cm^{-1}$, C=O stretching band of ester at 1746,

1727 $cm^{-1}$, C-H stretching of alkanes at 2914 $cm^{-1}$, O-H (intramolecular) stretching peak of hydroxyl at 3105 $cm^{-1}$, C=C (aromatic) stretching band at 1603 $cm^{-1}$, N-O stretching band of nitro at 1530 $cm^{-1}$, C-F stretching band is at 1251 $cm^{-1}$.

UV-vis (nm): 276 nm, 337 nm.

| Compound | M+H | M-H | Exact Mass | Observed Mass | % error |
|---|---|---|---|---|---|
| **16.F** | 755.3707 | 753.3551 | 754.3629 | 755.3745 | 0.0005 |

Compound **18.F**:

$^{1}$H NMR (400 MHz, $CDCl_3$, $\delta$ in ppm): $\delta$ = 13.24 (s, 1H, -OH), 8.55 (s, 1H, -CH=N-), 8.14 (d, 4H, *J*= 8.0 Hz Ar-H), 8.06 (d, 1H, *J* = 8.0 Hz, Ar-H), 7.53-7.41 (m, 3H, Ar-H), 7.32 (d, 1H, *J* = 8.0 Hz, Ar-H), 6.98 (d, 2H, *J* = 8.0 Hz, Ar-H), 6.92 (s, 1H, Ar-H), 6.87 (d, 1H, *J* = 8.0 Hz, Ar-H), 4.05 (t, 2H, *J* = 8.0 Hz, -$OCH_2$-), 2.68 (s, 3H, -$CH_3$), 1.86-1.79 (m, 2H, -$CH_2$), 1.51-1.44 (m, 2H, -$CH_2$), 1.36-1.24 (m, 28H, -$(CH_2)_{14}$), 0.88 (t, 3H, *J* = 4.0 Hz, -$CH_3$).

$^{13}$C NMR (100 MHz, $CDCl_3$, $\delta$ in ppm): $\delta$ = 14.14, 15.47, 22.70, 25.98, 29.08, 29.37,29.57, 29.60, 29.67, 29.71, 31.93,68.37, 110.77, 112.91, 113.15, 113.46, 114.36, 117.00, 120.24, 121.01, 123.58, 124.61, 126.89, 128.65, 129.26, 132.40, 133.43, 135.16, 143.74, 143.87, 145.84, 149.56, 152.51, 155.32, 162.51, 163.32, 163.64, 163.75, 164.33.

ATR ($cm^{-1}$): HC=N stretching of an imine at 1629 $cm^{-1}$, C=O stretching band of ester at 1752, 1720 $cm^{-1}$, C-H stretching of alkanes at 2914 $cm^{-1}$, O-H (intramolecular) stretching peak of hydroxyl at 3109 $cm^{-1}$, C=C (aromatic) stretching band at 1605 $cm^{-1}$, N-O stretching band of nitro at 1531 $cm^{-1}$, C-F stretching band is at 1261 $cm^{-1}$.

UV-vis (nm): 277 nm, 337 nm.

| Compound | M+H | M-H | Exact Mass | Observed Mass | % error |
|---|---|---|---|---|---|
| **18.F** | 783.4020 | 781.3864 | 782.3942 | 783.4048 | 0.00036 |

Compound **4.Cl**:

$^{1}$H NMR (400 MHz, $CDCl_3$, $\delta$ in ppm): $\delta$ = 13.25 (s, 1H, -OH), 8.56 (s, 1H, -CH=N-), 8.42 (s, 1H, Ar-H) 8.25 (d, 1H, *J*= 8.0 Hz Ar-H), 8.15-8.13 (m, 3H, Ar-H), 7.52-7.42 (m, 3H, Ar-H), 7.4 (d, 1H, *J* = 7.6 Hz, Ar-H), 6.98 (d, 2H, *J* = 8.0 Hz, Ar-H), 6.92 (s, 1H, Ar-H), 6.87 (d, 1H, *J* = 8.0 Hz, Ar-H), 4.06 (t, 2H, *J* = 6.0 Hz, -$OCH_2$-), 2.69 (s, 3H, -$CH_3$), 1.86-1.79 (m, 2H, -$CH_2$-), 1.55-1.48 (m, 2H, -$CH_2$), 1.00 (t, 3H, *J* = 8.0 Hz, -$CH_3$). (figure 15)

$^{13}$C NMR (100 MHz, $CDCl_3$, $\delta$ in ppm): $\delta$ = 13.84, 15.45, 19.19, 31.11, 68.04, 110.76, 113.45, 114.35, 117.00, 121.01, 123.23, 123.58, 124.63, 126.01, 126.90, 128.52, 128.71, 129.31, 132.40, 133.43, 135.26, 145.75, 149.55, 152.26, 155.31, 162.50, 163.30, 163.74, 164.33. (figure 16)

ATR ($cm^{-1}$): HC=N stretching of an imine at 1619 cm−1, C=O stretching band of ester at 1757, 1719 $cm^{-1}$, C-H stretching of alkanes at 2963 $cm^{-1}$, O-H(intramolecular) stretching peak of hydroxyl at 3104 $cm^{-1}$, C=C (aromatic) stretching band at 1607 $cm^{-1}$, N-O stretching band of nitro at 1522 $cm^{-1}$, C-Cl stretching band is at 739 $cm^{-1}$.

UV-vis (nm): 277 nm, 336 nm.

| **Compound** | **M+H** | **M-H** | **Exact Mass** | **Observed Mass** | **% error** |
|---|---|---|---|---|---|
| **4.Cl** | 603.1534 | 601.1378 | 602.1456 | 603.1563 | 0.00048 |

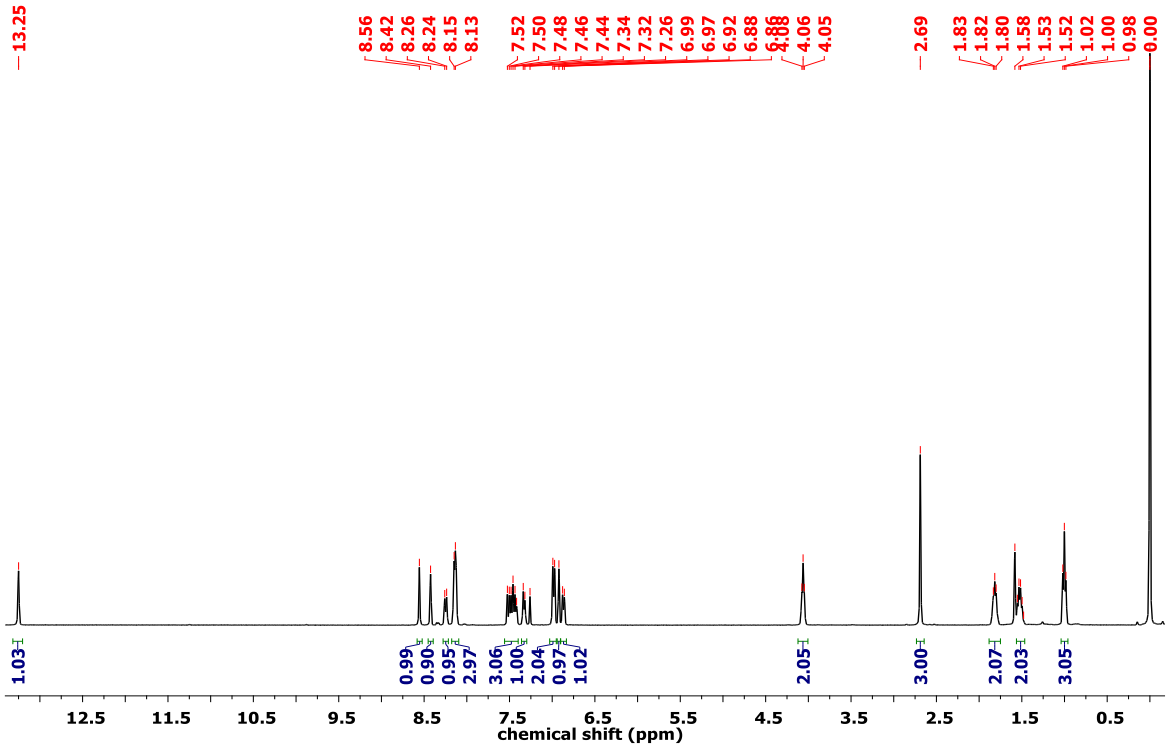


**Figure 15**: $^{1}$H NMR of compound **4.Cl**.

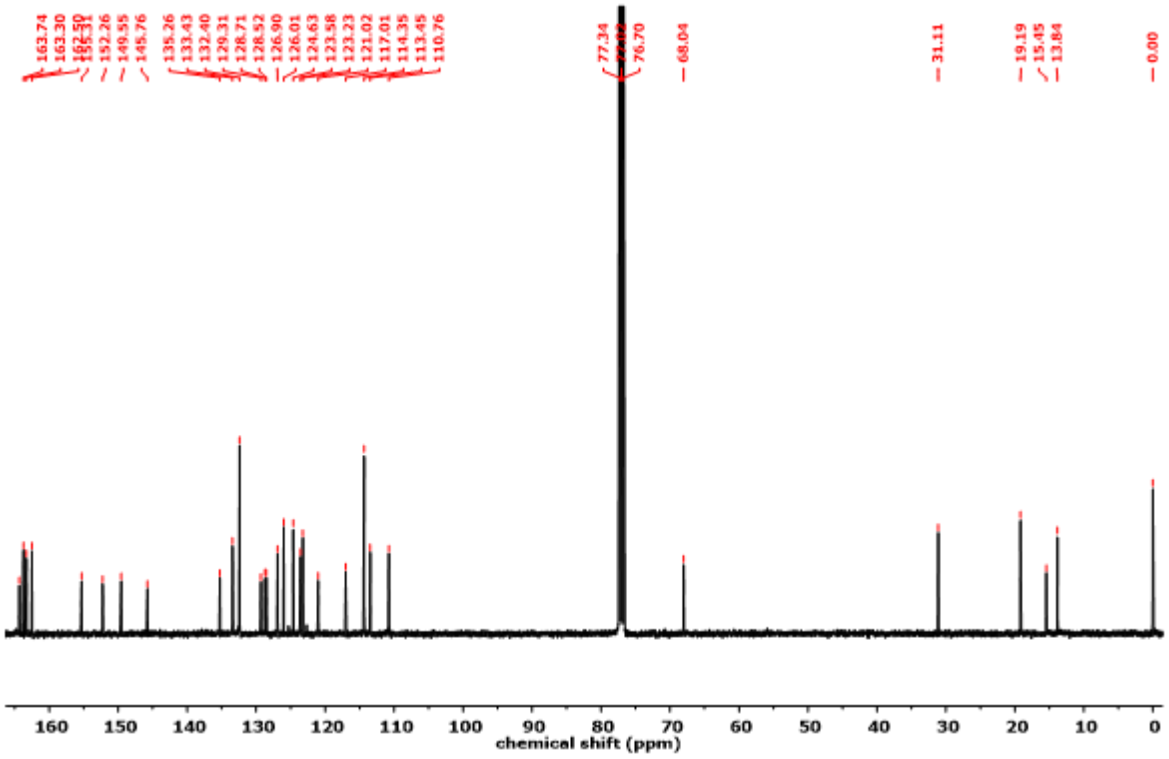


**Figure 16**:$^{13}$C NMR of compound **4.Cl**.

Compound **6.Cl**:

$^{1}$H NMR (400 MHz, $CDCl_3$, $\delta$ in ppm): $\delta$ = 13.26 (s, 1H, -OH), 8.56 (s, 1H, -CH=N-), 8.43 (d, 1H, J= 2.24, Ar-H)8.25 (dd, 1H, J = 8.0, 4.0 Hz, Ar-H), 8.16-8.13 (m, 3H, Ar-H), 7.53-7.42 (m, 3H, Ar-H), 7.33 (d, 1H, *J* = 8.0 Hz, Ar-H), 6.98 (d, 2H, *J* = 8.0 Hz, Ar-H), 6.92 (s, 1H, Ar-H), 6.87 (d, 1H, *J* = 8.0 Hz, Ar-H), 4.05 (t, 2H, *J* = 6.0 Hz, -$OCH_2$-), 2.69 (s, 3H, -$CH_3$), 1.86-1.79 (m, 2H, -$CH_2$-), 1.52-1.45 (m, 2H, -$CH_2$-), 1.39-1.33 (m, 4H, -$(CH_2)_2$-), 0.92 (t, 3H, *J* = 6.0 Hz, -$CH_3$).

$^{13}$C NMR (100 MHz, $CDCl_3$, $\delta$ in ppm): $\delta$ = 14.05, 15.46, 22.60, 25.66, 29.05, 31.55, 68.36, 110.77, 113.46, 114.36, 117.01, 121.02, 123.23, 123.60, 124.64, 126.03, 126.90, 128.54, 128.72, 129.32, 132.41, 133.43, 135.27, 145.77, 149.58, 152.27, 155.32, 162.51, 163.31, 163.74, 164.34.

ATR ($cm^{-1}$): HC=N stretching of an imine at 1619 $cm^{-1}$, C=O stretching band of ester at 1756, 1720 $cm^{-1}$, C-H stretching of alkanes at 2933 $cm^{-1}$, O-H (intramolecular) stretching peak of hydroxyl at 3103 $cm^{-1}$, C=C (aromatic) stretching band at 1607 $cm^{-1}$, N-O stretching band of nitro at 1525 $cm^{-1}$, C-Cl stretching band is at 740 $cm^{-1}$.

UV-vis (nm): 276 nm, 336 nm.

| Compound | M+H | M-H | Exact Mass | Observed Mass | % error |
|---|---|---|---|---|---|
| **6.Cl** | 631.1847 | 629.1691 | 630.1769 | 631.1872 | 0.00039 |

Compound **8.Cl**:

$^{1}$H NMR (400 MHz, $CDCl_3$, $\delta$ in ppm): $\delta$ = 13.26 (s, 1H, -OH), 8.56 (s, 1H, -CH=N-), 8.43 (d, 1H, *J* = 2.4, Ar-H), 8.25 (dd, 1H, *J* = 8.9, 2.4 Hz, Ar-H), 8.15-8.13 (m, 3H, Ar-H), 7.53-7.42 (m, 3H, Ar-H), 7.33 (d, 1H, *J* = 8.0 Hz, Ar-H), 6.98 (d, 2H, *J* = 8.0 Hz, Ar-H), 6.92 (s, 1H, Ar-H), 6.87 (dd, 1H, *J* = 8.38, 1.5 Hz, Ar-H), 4.05 (t, 2H, *J* = 8.0 Hz, -$OCH_2$-), 2.69 (s, 3H, -$CH_3$), 1.86-1.79 (m, 2H, -$CH_2$-), 1.52-1.44 (m, 2H, -$CH_2$-), 1.39-1.25 (m, 8H, -$(CH_2)_4$-), 0.90 (t, 3H, *J* = 6.0 Hz, -$CH_3$).

$^{13}$C NMR (100 MHz, $CDCl_3$, $\delta$ in ppm): $\delta$ = 14.12, 15.46, 22.67, 25.98, 29.08, 29.23, 29.33, 31.81, 68.37, 110.77, 113.46, 114.36, 117.01, 121.01, 123.23, 123.59, 124.63, 126.02, 126.90, 128.53,

128.72, 129.32, 132.40, 133.43, 135.27, 145.76, 149.57, 152.27, 155.32, 162.51, 163.31, 163.74, 164.34.

ATR ($cm^{-1}$): HC=N stretching of an imine at 1621 $cm^{-1}$, C=O stretching band of ester at 1748, 1717 $cm^{-1}$, C-H stretching of alkanes at 2924 $cm^{-1}$, O-H (intramolecular) stretching peak of hydroxyl at 3103 $cm^{-1}$, C=C (aromatic) stretching band at 1612 $cm^{-1}$, N-O stretching band of nitro at 1517 $cm^{-1}$, C-Cl stretching band is at 743 $cm^{-1}$.

UV-vis (nm): 277 nm, 336 nm.

| **Compound** | **M+H** | **M-H** | **Exact Mass** | **Observed Mass** | **% error** |
|---|---|---|---|---|---|
| **8.Cl** | 659.2160 | 657.2004 | 658.2082 | 659.2191 | 0.00047 |

Compound **10.Cl**:

$^{1}$H NMR (400 MHz, $CDCl_3$, $\delta$ in ppm): $\delta$ = 13.26 (s, 1H, -OH), 8.56 (s, 1H, -CH=N-), 8.43 (d, 1H, *J* = 2.46 Hz Ar-H), 8.25 (dd, 1H, *J* = 8.9, 2.4 Hz, Ar-H), 8.15-8.13 (m, 3H, Ar-H), 7.53-7.42 (m, 3H, Ar-H), 7.33 (d, 1H, *J* = 8.0 Hz, Ar-H), 6.98 (d, 2H, *J* = 8.0 Hz, Ar-H), 6.92 (s, 1H, Ar-H), 6.87 (d, 1H, *J* = 8.0 Hz, Ar-H), 4.05 (t, 2H, *J* = 8.0 Hz, -$OCH_2$-), 2.69 (s, 3H, -$CH_3$), 1.86-1.79 (m, 2H, -$CH_2$-), 1.51-1.44 (m, 2H, -$CH_2$-), 1.38-1.28 (m, 12H, -$(CH_2)_6$-), 0.89 (t, 3H, *J* = 6.0 Hz, -$CH_3$).

$^{13}$C NMR (100 MHz, $CDCl_3$, $\delta$ in ppm): $\delta$ = 14.14, 15.46, 22.69, 25.98, 29.08, 29.32, 29.36, 29.56, 31.90, 68.37, 110.77, 113.46, 114.36, 117.01, 121.01, 123.23, 123.59, 124.63, 126.02, 126.90, 128.53, 128.72, 129.32, 132.40, 133.43, 135.27, 145.77, 149.58, 152.27, 155.32, 162.51, 163.31, 163.74, 164.34.

ATR ($cm^{-1}$): HC=N stretching of an imine at 1621 $cm^{-1}$, C=O stretching band of ester at 1752, 1722 $cm^{-1}$, C-H stretching of alkanes at 2923 $cm^{-1}$, O-H (intramolecular) stretching peak of hydroxyl at 3103 $cm^{-1}$, C=C (aromatic) stretching band at 1610 $cm^{-1}$, N-O stretching band of nitro at 1526 $cm^{-1}$, C-Cl stretching band is at 741 $cm^{-1}$.

UV-vis (nm): 277 nm, 336 nm.

| Compound | M+H | M-H | Exact Mass | Observed Mass | % error |
|---|---|---|---|---|---|
| **10.Cl** | 687.2473 | 685.2317 | 686.2395 | 687.2499 | 0.00038 |

Compound **12.Cl**:

$^{1}$H NMR (400 MHz, $CDCl_3$, $\delta$ in ppm): $\delta$ = 13.26 (s, 1H, -OH), 8.56 (s, 1H, -CH=N-), 8.43 (d, 1H, *J* = 2.4 Hz, Ar-H), 8.25 (dd, 1H, *J* = 8.9, 2.36 Hz, Ar-H), 8.15-8.13(m, 3H, Ar-H), 7.53-7.42 (m, 3H, Ar-H), 7.33 (d, 1H, *J* = 8.0 Hz, Ar-H), 6.98 (d, 2H, *J* = 8.0 Hz, Ar-H), 6.92 (s, 1H, Ar-H), 6.87 (d, 1H, *J* = 8.0 Hz, Ar-H), 4.05 (t, 2H, *J* = 8.0 Hz, -$OCH_2$-), 2.69 (s, 3H, -$CH_3$), 1.86-1.79 (m, 2H, -$CH_2$-), 1.51-1.44 (m, 2H, -$CH_2$-), 1.38-1.27 (m, 16H, -$(CH_2)_8$-), 0.88 (t, 3H, *J* = 6.0 Hz, -$CH_3$).

$^{13}$C NMR (100 MHz, $CDCl_3$, $\delta$ in ppm): $\delta$ = 14.14, 15.46, 22.70, 25.98, 29.08, 29.36, 29.57, 29.60, 29.64, 29.66, 31.92, 68.37, 110.77, 113.46, 114.36, 117.01, 121.01, 123.23, 123.59, 124.64, 126.02, 126.90, 128.53, 128.72, 129.32, 132.41, 133.43, 135.27, 145.77, 149.58, 152.27, 155.32, 162.51, 163.31, 163.75, 164.34.

ATR ($cm^{-1}$): HC=N stretching of an imine at 1621 $cm^{-1}$, C=O stretching band of ester at 1753, 1723 $cm^{-1}$, C-H stretching of alkanes at 2916 $cm^{-1}$, O-H (intramolecular) stretching peak of hydroxyl at 3107 $cm^{-1}$, C=C (aromatic) stretching band at 1606 $cm^{-1}$, N-O stretching band of nitro at 1523 $cm^{-1}$, C-Cl stretching band is at 734 $cm^{-1}$.

UV-vis (nm): 277 nm, 336 nm.

| Compound | M+H | M-H | Exact Mass | Observed Mass | % error |
|---|---|---|---|---|---|
| **12.Cl** | 715.2786 | 713.2630 | 714.2708 | 715.2812 | 0.00013 |

Compound **14.Cl**:

$^{1}$H NMR (400 MHz, $CDCl_3$, $\delta$ in ppm): $\delta$ = 13.26 (s, 1H, -OH), 8.56 (s, 1H, -CH=N-), 8.43 (d, 1H, *J* = 2.4 Hz, Ar-H), 8.25 (dd, 1H, *J* = 8.8, 2.4 Hz, Ar-H), 8.15-8.13 (m, 3H, Ar-H), 7.53-7.42 (m, 3H, Ar-H), 7.33 (d, 1H, *J* = 8.0 Hz, Ar-H), 6.98 (d, 2H, *J* = 8.0 Hz, Ar-H), 6.92 (s, 1H, Ar-

H), 6.87 (d, 1H, *J* = 8.0 Hz, Ar-H), 4.05 (t, 2H, *J* = 8.0 Hz, -$OCH_2$-), 2.69 (s, 3H, -$CH_3$), 1.86-1.79 (m, 2H, -$CH_2$-), 1.51-1.44 (m, 2H, -$CH_2$-), 1.38-1.27 (m, 20H, -$(CH_2)_{10}$-), 0.88 (t, 3H, *J* = 8.0 Hz, -$CH_3$).

$^{13}$C NMR (100 MHz, $CDCl_3$, $\delta$ in ppm): $\delta$ = 14.14, 15.46, 22.70, 25.98, 29.08, 29.37, 29.56, 29.60, 29.66, 29.68, 29.70, 31.93, 68.37, 110.77, 113.46, 114.36, 117.01, 121.01, 123.23, 123.59, 124.63,

126.02, 126.90, 128.53, 128.72, 129.32, 132.40, 133.43, 135.27, 145.77, 149.57, 152.27, 155.32, 162.51, 163.31, 163.75, 164.34.

ATR ($cm^{-1}$): HC=N stretching of an imine at 1620 $cm^{-1}$, C=O stretching band of ester at 1749, 1719 $cm^{-1}$, C-H stretching of alkanes at 2916 $cm^{-1}$, O-H (intramolecular) stretching peak of hydroxyl at 3107 $cm^{-1}$, C=C (aromatic) stretching band at 1608 $cm^{-1}$, N-O stretching band of nitro at 1518 $cm^{-1}$, C-Cl stretching band is at 736 $cm^{-1}$.

UV-vis (nm): 276 nm, 337 nm.

| **Compound** | **M+H** | **M-H** | **Exact Mass** | **Observed Mass** | **% error** |
|---|---|---|---|---|---|
| **14.Cl** | 743.3099 | 741.2943 | 742.3021 | 743.3126 | 0.00036 |

Compound **16.Cl**:

$^{1}$H NMR (400 MHz, $CDCl_3$, $\delta$ in ppm): $\delta$ = 13.26 (s, 1H, -OH), 8.56 (s, 1H, -CH=N-), 8.43 (s, 1H, Ar-H), 8.25 (d, 1H, *J* = 8.0 Hz, Ar-H), 8.15-8.13 (m, 3H, Ar-H), 7.53-7.42 (m, 3H, Ar-H), 7.33 (d, 1H, *J* = 8.0 Hz, Ar-H), 6.98 (d, 2H, *J* = 8.0 Hz, Ar-H), 6.92 (s, 1H, Ar-H), 6.87 (d, 1H, *J* = 8.0 Hz, Ar-H), 4.05 (t, 2H, *J* = 8.0 Hz, -$OCH_2$-), 2.69 (s, 3H, -$CH_3$), 1.86-1.79 (m, 2H, -$CH_2$-), 1.51-1.44 (m, 2H, -$CH_2$-), 1.37-1.26 (m, 24H, -$(CH_2)_{12}$-), 0.88 (t, 3H, *J* = 8.0 Hz, -$CH_3$).

$^{13}$C NMR (100 MHz, $CDCl_3$, $\delta$ in ppm): $\delta$ = 14.14, 15.46, 22.71, 25.98, 29.09, 29.37, 29.57, 29.60, 29.67, 29.70, 31.93, 68.37, 110.77, 113.46, 114.36, 117.01, 121.02, 123.23, 123.59, 124.63, 126.02, 126.90, 128.53, 128.72, 129.32, 132.40, 133.43, 135.27, 145.77, 149.57, 152.27, 155.32, 162.51, 163.31, 163.75, 164.33.

ATR ($cm^{-1}$): HC=N stretching of an imine at 1621 $cm^{-1}$, C=O stretching band of ester at 1756,

1721 $cm^{-1}$, C-H stretching of alkanes at 2912 $cm^{-1}$, O-H (intramolecular) stretching peak of hydroxyl at 3107 $cm^{-1}$, C=C (aromatic) stretching band at 1609 $cm^{-1}$, N-O stretching band of nitro at 1525 $cm^{-1}$, C-Cl stretching band is at 739 $cm^{-1}$.

UV-vis (nm): 277 nm, 336 nm.

| Compound | M+H | M-H | Exact Mass | Observed Mass | % error |
|---|---|---|---|---|---|
| **16.Cl** | 771.3412 | 769.3256 | 770.3334 | 771.3439 | 0.00035 |

Compound **18.Cl**:

$^{1}$H NMR (400 MHz, $CDCl_3$, $\delta$ in ppm): $\delta$ = 13.26 (s, 1H, -OH), 8.56 (s, 1H, -CH=N-), 8.43 (s, 1H, Ar-H) 8.23 (d, 1H, J= 8.0 Hz Ar-H), 8.15-8.13 (m, 3H, Ar-H), 7.53-7.42 (m, 3H, Ar-H), 7.33 (d, 1H, *J* = 8.0 Hz, Ar-H), 6.98 (d, 2H, *J* = 8.0 Hz, Ar-H), 6.92 (s, 1H, Ar-H), 6.87 (d, 1H, *J* = 8.0 Hz, Ar-H), 4.05 (t, 2H, *J* = 8.0 Hz, -$OCH_2$-), 2.69 (s, 3H, -$CH_3$), 1.86-1.79 (m, 2H, -$CH_2$-), 1.51-1.44 (m, 2H, -$CH_2$-), 1.38-1.26 (m, 28H, -$(CH_2)_{14}$), 0.88 (t, 3H, *J* = 8.0 Hz, -$CH_3$).

$^{13}$C NMR (100 MHz, $CDCl_3$, $\delta$ in ppm): $\delta$ = 14.14, 15.46, 22.70, 25.98, 29.09, 29.37, 29.57, 29.60, 29.67, 29.71, 31.93, 68.37, 110.76, 113.45, 114.36, 117.01, 121.01, 123.23, 123.58, 124.63, 126.02, 126.90, 128.53, 128.72, 129.32, 132.40, 133.43, 135.26, 145.76, 149.57, 152.27, 155.32, 162.51, 163.30, 163.75, 164.33.

ATR ($cm^{-1}$): HC=N stretching of an imine at 1623 $cm^{-1}$, C=O stretching band of ester at 1747, 1730 $cm^{-1}$, C-H stretching of alkanes at 2916 $cm^{-1}$, O-H (intramolecular) stretching peak of hydroxyl at 3106 $cm^{-1}$, C=C (aromatic) stretching band at 1605 $cm^{-1}$, N-O stretching band of nitro at 1513 $cm^{-1}$, C-Cl stretching band is at 740 $cm^{-1}$.

UV-vis (nm): 276 nm, 336 nm.

| Compound | M+H | M-H | Exact Mass | Observed Mass | % error |
|---|---|---|---|---|---|
| **18.Cl** | 799.3725 | 797.3569 | 798.3647 | 799.3759 | 0.00042 |

## ATR studies

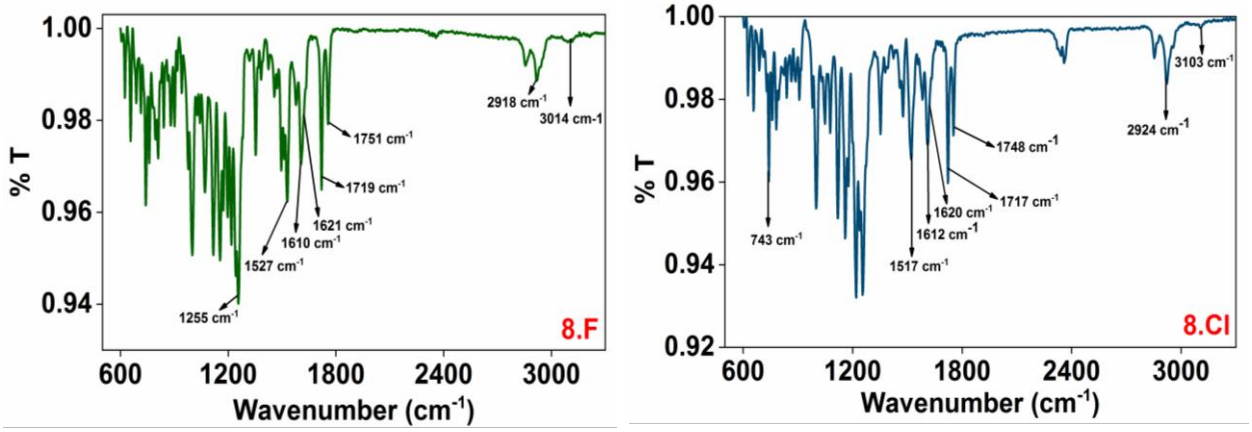


**Figure 17**: ATR spectra of two representative compounds **8.F** and **8.Cl**.

## UV-visible studies

In order to acquire information about absorption maxima of compounds, the UV absorption spectroscopic studies were carried out on the representative **4.F** and **4.Cl** compounds from both the series in dichloromethane ($CH_2Cl_2$) solution of $10^{-4}$ M concentration. The compounds exhibited a maximum absorption peak at ~ 276 nm (4.49 eV, ε ~ 10,000 $Lmol^{-1}cm^{-1}$) and minimum absorption peak at ~ 337 nm (Figure 18a). The absorption band with large molar absorption coefficient ($\lambda_{max}$ ~ 276 nm) coincides with the π-π* transition of the highly π-conjugated system with substituted phenyl benzoate unit as the core. Similar results were found for the other homologous of **4.F** and **4.Cl** series (where n = 6, 8, 10, 12, 14, 16, 18) as well.

The plot of the absorption spectra follows no trend as such upon altering the alkyl chain in a particular series (**n.F** or **n.Cl**) as shown in Figure 18 (b,c).

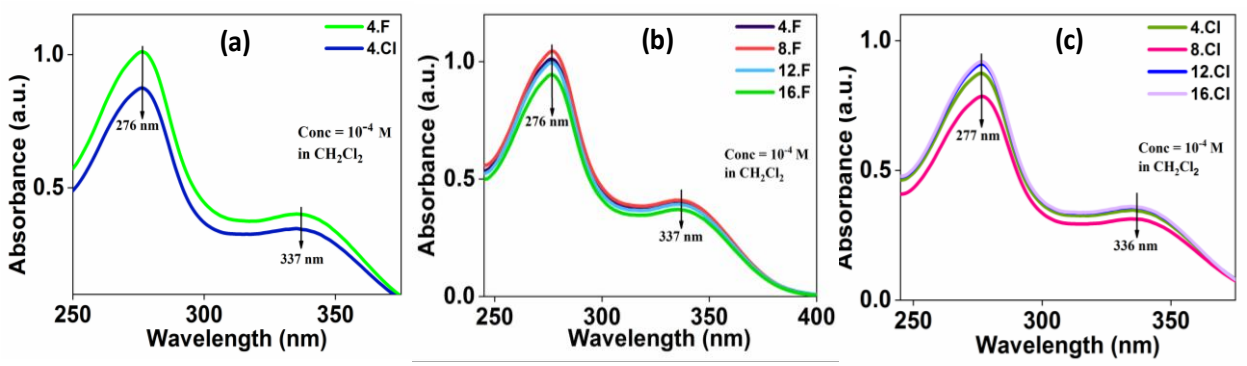


**Figure 18**: (a) Comparative UV-vis spectra of two compounds **4.F** and **4.Cl**, (b,c) effect of variation of alkyl chain on absorbance and wavelength for series **n.F** and **n.Cl** respectively.

### 2.2.3 Material characterization

The mesogenic behaviour of all the compounds of series **n.F** and **n.Cl** is characterized by Polarising Optical Microscopy (POM) studies and further confirmed by Differential Scanning Calorimetry (DSC) studies.

#### 2.2.3.1 Polarizing Optical Microscopy (POM) studies:

The mesomorphic properties of the compounds were characterized with the help of POM technique. The solid sample was placed in a glass plate, heated up to its isotropic temperature, covered with a transparent cover slip and observed under the microscope (polarizer and analyzer at 90°). The compounds were birefringent indicating their liquid crystalline behavior. Upon cooling from the isotropic phase (at 10 °C $min^{-1}$), a birefringent schlieren texture for Nematic phase appeared for compound **8.F** at 163.0 °C (Figure 19c) which fully grew into a Nematic phase upon decreasing temperature and finally crystallized at 92.0 °C. Similar behavior (i.e. N phase) was observed for all the lower homologues of series **n.F** and **n.Cl** (n = 4, 6, 8) as shown in Figure 19 (a,b,e). The higher homologues (n = 14, 16, 18) of both the series exhibited enantiotropic Smectic A phase depicted mainly by fan-like texture (Figure 19 (g-i)) and other characteristic textures (Figure 19 (d,f)). The intermediate chain homologues (n = 10, 12) of both the series exhibited both N as well as SmA phase except **12.F** which showed only monotropic SmA phase.

The isotropic temperature was found to be in the range ~ 175-196 °C for **n.F** series and ~ 145-178 °C for **n.Cl** series.

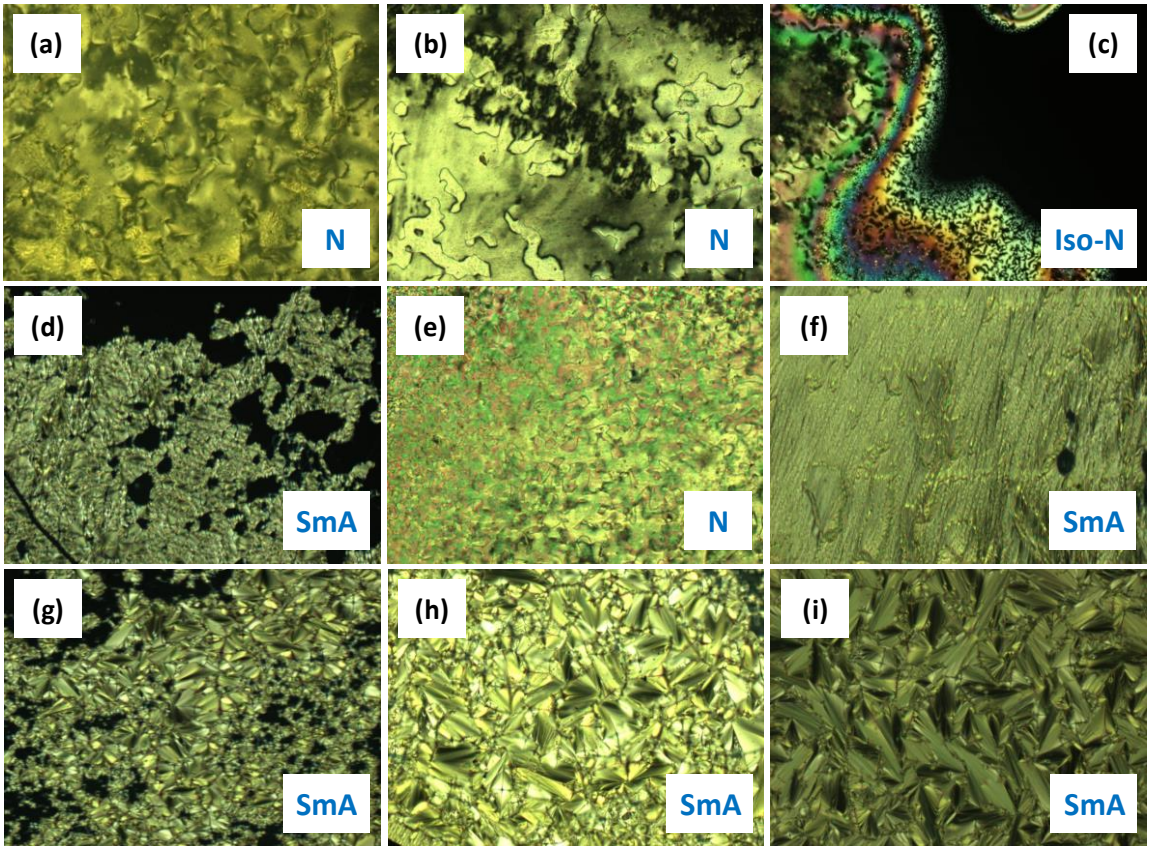


**Figure 19**: Polarizing optical micrographs of some representative compounds under crossed polarizers in a 2.5 μm normal cell of (a) **4.F** at 151.0 °C, (b) **6.Cl** at 140.0 °C, (c) **8.F** at 163.0 °C, (d) **10.F** at 123.0 °C, (e) **10.Cl** at 149.3 °C, (f) **10.Cl** at 125.6 °C, (g) **14.Cl** at 146.5 °C, (h) **16.F** at 160.0 °C, (h) **18.Cl** at 126.0 °C upon cooling (rate: 10 °C $min^{-1}$).

### 2.2.3.2 Differential Scanning Calorimetry (DSC) studies:

To verify the POM observations, DSC studies were carried out to determine the exact transition temperatures for different phases and also the enthalpies of those phases. All the compounds are enantiotropic in nature i.e. exhibit mesophases upon both heating and cooling. These transition

temperatures and associated enthalpies; phase range of Nematic, Smectic and total mesophase (N and SmA) for all the compounds of **n.F** and **n.Cl** series are presented have been presented in Table 1 and Table 2 respectively. The DSC spectra have been plotted for all the compounds of **n.F** and **n.Cl** series are presented in Figure 20 and Figure 21 respectively.

**Table 1**: Phase transition temperatures and thermal range (Nematic, Smectic A and total mesophase range calculated upon cooling) of all the compounds of **n.F** series recorded for heating (first row) and cooling (second row) cycles at 10 °C $min^{-1}$.

| n.F | Phase transition temperatures (ΔH in kJ $mol^{-1}$) | N range (°C) | SmA range (°C) | Total mesophase range (°C) |
|---|---|---|---|---|
| **4.F** | Cr 139.24 °C (29.9) N 196.06 °C (0.11) Iso<br>Iso 192.69 °C (-0.1) N 91.30 °C (-22.5) Cr | 101.39 | | 101.39 |
| **6.F** | Cr 123.86 °C (30.7) N 184.05 °C (0.24) Iso<br>Iso 180.25 °C (-0.15) N 93.56 °C (-26.6) Cr | 86.69 | | 88.69 |
| **8.F** | Cr 114.51 °C (19.7) N 166.91 °C (0.2) Iso<br>Iso 163.38 °C (-0.1) N 91.13 °C (-24.4) Cr | 72.25 | | 72.25 |
| **10.F** | Cr 118.08 °C (31.4) SmA[a]139.3°C N 170.49 °C (0.08) Iso<br>Iso 166.83 °C (-0.07) N 139.5°CSmA[a] 93.56 °C (-31.4) Cr | 27.33 | 45.94 | 73.27 |
| **12.F** | Cr 108.66 °C (14.4) SmA 153.35 °C (0.4) Iso<br>Iso 142.25 °C (-0.3) SmA 88.83 °C (-23.8) Cr | | 53.42 | 53.42 |
| **14.F** | Cr 110.75 °C (18.9) SmA 168.91 °C (1.93) Iso<br>Iso 165.90 °C (-2.4) SmA 93.85 °C (-19.9) Cr | | 72.05 | 72.05 |
| **16.F** | Cr 112.56 °C (10.9) SmA 175.13 °C (1.3) Iso<br>Iso 172.20 °C (-1.3) SmA 90.43 °C (-12.04) Cr | | 81.77 | 81.77 |
| **18.F** | Cr 112.40 °C (19.1) SmA 175.47 °C (3.8) Iso<br>Iso 172.38 °C (-3.2) SmA 89.78 °C (-20.7) Cr | | 82.60 | 82.60 |

[a]SmA phase not observed by DSC but POM and XRD.

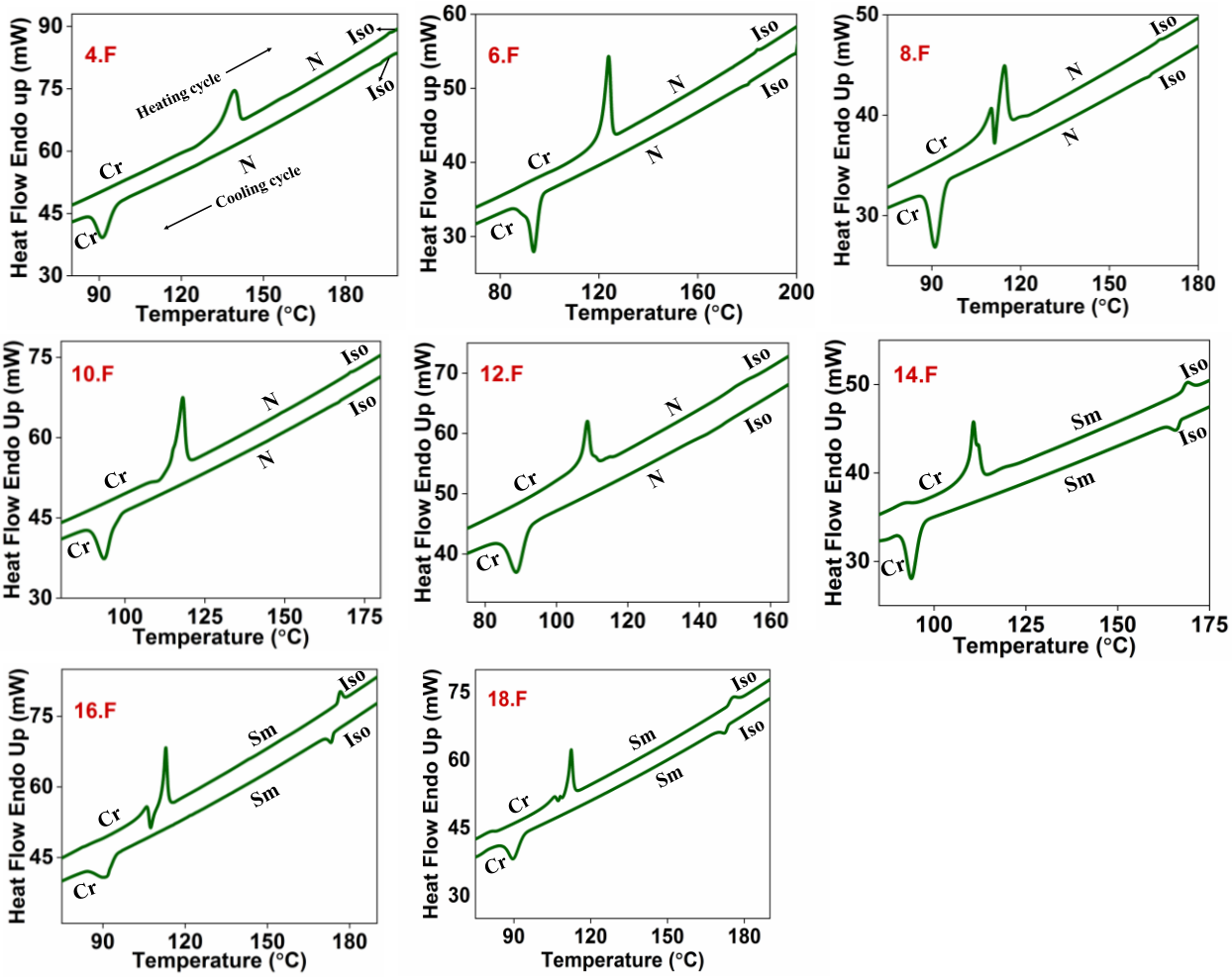


**Figure 20**: DSC thermographs (both heating and cooling cycles) of all the final compounds of series **n.F** recorded at 10 °C $min^{-1}$.

**Table 2**: Phase transition temperatures and thermal range (Nematic, Smectic A and total mesophase range calculated upon cooling) of all the compounds of **n.Cl** series recorded for heating (first row) and cooling (second row) cycles at 10 °C $min^{-1}$.

| n.Cl | Phase transition temperatures (ΔH in kJ $mol^{-1}$) | N range (°C) | SmA range (°C) | Total mesophase range (°C) |
|---|---|---|---|---|
| **4.Cl** | Cr 146.16 °C (15.8) N 178.07 °C (0.1) Iso<br>Iso 171.35 °C (-0.08) N 117.66 °C (-24.2) Cr | 53.69 | | 53.69 |
| **6.Cl** | Cr 137.31 °C (12.8) N 168.29 °C (0.10) Iso<br>Iso 162.40 °C (-0.04) N 112.98 °C (-15.4) Cr | 42.42 | | 42.42 |
| **8.Cl** | Cr 134.85 °C (26.9) N 157.25 °C (0.1) Iso<br>Iso 150.78 °C (-0.1) N 112.15 °C (19.7) Cr | 38.63 | | 38.63 |
| **10.Cl** | Cr 133.67 °C (22.5) N 154.72 °C (0.2) Iso<br>Iso 150.26 °C (-0.1) N 130.0°C SmA[a]113.73°C (-19.1) Cr | 20.26 | 16.27 | 36.53 |
| **12.Cl** | Cr 135.42 °C (21.05) SmA 150.33 °C (0.09) N 154.72 °C (0.2) Iso<br>Iso 150.25 °C (-0.17) N 145.88 °C (-0.08) SmA 118.70°C (-26.3) Cr | 4.37 | 27.18 | 31.55 |
| **14.Cl** | Cr 136.39 °C (27.9) SmA 159.22 °C (2.2) Iso<br>Iso 154.72 °C (-1.3) SmA 116.32 °C (-29.2) Cr | | 38.40 | 38.40 |
| **16.Cl** | $Cr_1$ 94.2 °C (4.32) $Cr_2$ 134.4 °C (23.77) SmA 159.9 °C (2.43) Iso<br>Iso 154.5 °C (-2.44) SmA 113.4 °C $Cr_2$ (-26.7) 87.9 °C (-1.65) $Cr_1$ | | 41.40 | 41.40 |
| **18.Cl** | Cr 127.25 °C (15.01) SmA 144.86 °C (2.14) Iso<br>Iso 139.01 °C (-0.4) SmA 98.56 °C (-14.6) Cr | | 40.45 | 40.45 |

[a]SmA phase not observed by DSC but POM and XRD.

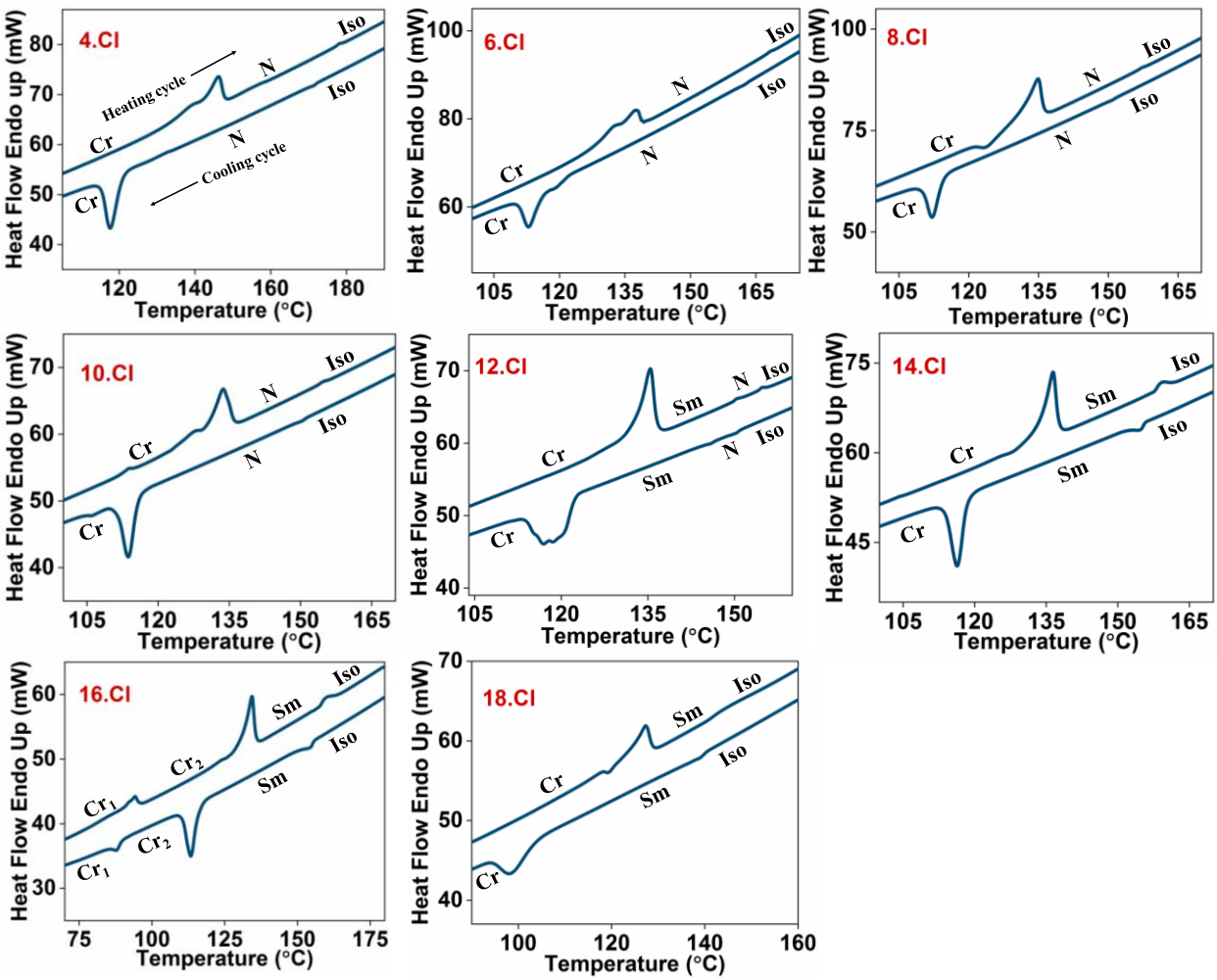


**Figure 21**: DSC thermographs (both heating and cooling cycles) of all the final compounds of series **n.Cl** recorded at 10 °C $min^{-1}$.

### 2.2.3.3 Structure-property relationship:

It has been found that the terminal fluoro moiety (series **n.F**) is more susceptible to induce the LC nature in these bent-core molecules as compared to the terminal chloro moiety (series **n.Cl**) i.e. the mesophase range for **n.F** series is almost twice as for **n.Cl** series (as observed upon cooling). As the alkyl chain increases (n = 6-12), the N phase range decreases for both the **n.F** and **n.Cl** series (Figure 22a). This trend is reversed in the case for SmA phase i.e. phase range increases as moving towards the higher homologues (n = 10-18) as shown in Figure 22b. Compound **12.F**

doesn’t show N phase but only SmA phase. The maximum N phase range has been observed in compound **4.F** (~ 101 °C) whereas **18.F** (~ 82 °C) displayed the maximum SmA phase range.

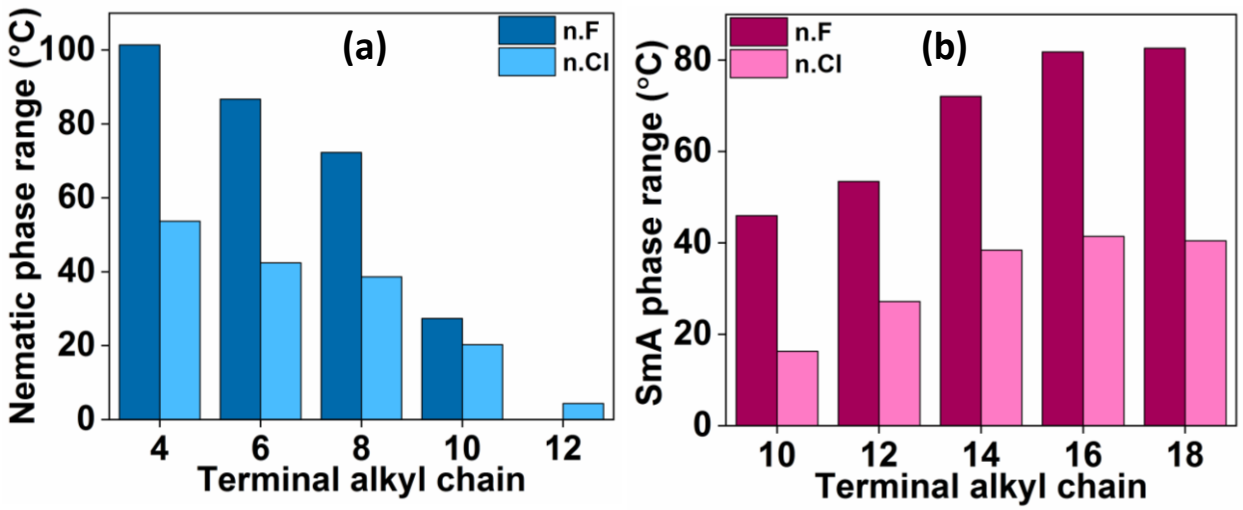


**Figure 22**: Variation of terminal alkyl chain with (a) N phase range and (b) SmA phase range (phase range observed for the cooling cycle in °C).

# Conclusions and Future Outlook

In summary, we have synthesized and characterized two series (**n.F** and **n.Cl**) of achiral hockey stick-shaped mesogens with different lateral halogen substitutions (F, Cl) at the terminal polar ring for the purpose of studying the structure-property relationship. All intermediates and final compounds have been structurally characterized with the help of NMR ($^{1}$H and $^{13}$C), ATR, ESI, and UV-vis spectroscopic techniques.

The final compounds of both the series were liquid crystalline i.e. exhibited enantiotropic mesomorphic behaviour (Nematic and Smectic A) phase as observed by POM studies and further confirmed by DSC studies. It has been found that the terminal fluoro moiety (series **n.F**) is more susceptible to induce the LC nature in these bent-core molecules as compared to the terminal chloro moiety (series **n.Cl**) i.e. the mesophase range for **n.F** series is almost twice as for **n.Cl** series. The maximum N and SmA phase range has been observed by compounds of **n.F** series i.e. **4.F** (~ 101 °C of N phase) and **18.F** (~ 82 °C of SmA phase).

The future work includes the pending studies:

(a) for further confirmation of nature of mesophases: Small/wide-angle X-ray Diffraction studies.

(b) to calculate the bent angle of these hockey-stick shaped molecules: Theoretical calculations (DFT studies).

# Bibliography


[1] Niori, T.; Sekine, T.; Watanabe, J.; Furukawa, T.; Takezoe, H. Distinct ferroelectric smectic liquid crystals consisting of banana shaped achiral molecules. *J. Mater. Chem.* **1996**, 6, 1231-1233.

[2] Akutagawa, T.; Matsunaga, Y.; Yasuhara, K. Mesomorphic behavior of 1,3-phenylene bis[4-(4- alkoxyphenyliminomethyl)benzoates] and related compounds. *Liq. Cryst.* **1994**, 17, 659-666.

[3] Jakli, A.; Lavrentovich, O. D.; Selinger, J. V. Physics of liquid crystals of bent-shaped molecules. *Rev. Mod. Phys.* **2018**, 90, 045004 (1-68).

[4] Kumar, S.; Gowda, A. N. The chemistry of bent-core molecules forming nematic liquid crystals. *Liquid Crystals Reviews.* **2015**, 3, 99-145.

[5] Amaranatha Reddy, R. A.; Tschierske, C. Bent-core liquid crystals: polar order, superstructural chirality and spontaneous desymmetrisation in soft matter systems. *J. Mater. Chem.* **2006**, 16, 907-961.

[6] Hough, L. E.; Jung, H. T.; Kruerke, D.; Heberling, M. S.; Nakata, M.; Jones, C. D.; Chen, D.; Link, D. R.; Zasadzinski, J.; Heppke, G.; Rabe, J. P.; Stocker, W.; Korblova, E.; Walba, D. M.; Glaser, M. A.; Clark, N. A. Helical Nanofilament Phases. *Science.* **2009**, 325, 456-460.

[7] Harden,J.; Chambers, M.; Verduzco, R.; Luchette, P.; Gleeson, J. T.; Sprunt, S.; Jakli, A. Giant flexoelectricity in bent-core nematic liquid crystal elastomers. *App. Phys. Lett*. **2010**, 96, 102907 (1-3).

[8] Pelzl, G.; Eremin, A.; Diele, S.; Kresse, H.; Weissflog, W. Spontaneous chiral ordering in the nematic phase of an achiral banana-shaped compound. *J. Mater. Chem.* **2002**, 12, 2591-2593.

[9] Kodre, K. V.; Attarde, S. R.; Yendhe, P. R.; Barge, V. U. Differential Scanning Calorimetry: A Review. *RRJPA*. **2014**, 3, 11-22.

[10] Kaur, S.; Mohiuddin, G.; Satapathy, P.; Nandi, R.; Punjani, V.; Prasad, S. K.; Pal, S. K. Influence of terminal halogen moieties on the phase structure of short-core achiral hockey-stick-shaped mesogens: design, synthesis and structure-property relationship. *Mol. Syst. Des. Eng.* **2018**, 3, 839-852.

[11] Nath, R. K.; Deb, R.; Chakraborty, N.; Mohiuddin, G.; Rao, D. S. S.; Rao, N. V. S. Influence of the chloro substituent on the mesomorphism of unsymmetrical achiral four-ring bent-core compounds: 2D polarization modulated banana phases. *J. Mater. Chem. C*. **2013,** 1**,** 663-670.

[12] Gude, V.; Upadhyaya, K.; Mohiuddin, G.; Rao, N. V. S. A new family of four-ring bent-core nematic liquid crystals with a highly polar end-group. *Liq. Cryst.* **2013**, 40, 1, 120-129.

[13] Somen Debnath, Golam Mohiuddin, Srikanth Turlapati, Nazma Begum, Dipika Debnath, Sarkar, N. V. S. Rao. Nematic phases in achiral unsymmetrical four-ring bent-core azo compounds possessing strongly polar cyano and nitro moieties as end substituents: Synthesis and characterization. *Dyes and Pigments.* **2013**, 99, 447-455.

[14] Paul, M. K.; Kalita, G.; Laskar, A. R.; Debnath, S.; Gude, V.; Sarkar, D. D.; Mohiuddin, G.; Varshney, S. K.; Rao, N. V. S. Synthesis and mesomorphic behaviour of achiral four-ring unsymmetrical bent-core liquid crystals: Nematic phases. *Journal of Molecular Structure.* **2013**, 1049, 78-89.

[15] Chakraborty, L.; Chakraborty, N.; Sarkar, D. D.; Rao, N. V. S.; Aya, S.; Le, K. V.; Araoka, F.; Ishikawa, K.; Pociecha, D., Gorecka, E.; Takezoe, H. Unusual temperature dependence of smectic layer structure associated with the nematic-smectic C phase transition in a hockey-stick-shaped four-ring compound. *J. Mater. Chem. C.* **2013**, 1, 1562-1566.